Synthesis and Spectroscopic Characterization of Some New [tris(3,5-dimethyl-pyrazol)borato] Molybdenum Complexes

By

Seçkiner DÜLGER İRDEM

A Dissertation Submitted to the
Graduate School in Partial Fulfillment of the
Requirements for the Degree of

MASTER OF SCIENCE

Department: Chemistry
Major: Chemistry

İzmir Institute of Technology
İzmir, Turkey

December, 2003

We approve the thesis of **Seçkiner DÜLGER İRDEM**

Date of Signature

....   **16.12.2003**

Assoc. Prof. Işıl TOPALOĞLU SÖZÜER

Thesis Adviser

Department of Chemistry

....   **16.12.2003**

Prof. Dr. Fadime UĞUR

Ege University, Faculty of Science

Department of Chemistry

....   **16.12.2003**

Prof. Dr. Tamerkan ÖZGEN

Department of Chemistry

....   **16.12.2003**

Prof. Dr. Levent ARTOK

Head of Department

ACKNOWLEDGEMENTS

ABSTRACT

In this study, the new binuclear oxo bridged imido Mo(V) complexes [MoTp*(O)Cl](μ-O)[MoTp*(Cl)(≡NC$_6$H$_4$X)], (p-X = Cl, Br) and [MoTp*(O)Cl](μ-O) [MoTp*(Cl)(≡NC$_6$H$_4$Y)], (m-Y = I, F) have been synthesized by the reaction oxo molybdenum (V) precursor [MoTp*(O)Cl$_2$]; [Tp* = Tris(3, 5-dimethyl-pyrazol)borato] with p- and m- functionalized anilines, H$_2$NC$_6$H$_4$X and H$_2$NC$_6$H$_4$Y (p-X = Cl, Br; m-Y=I, F) in toluene solution.

The complexes have been characterised by ^{1}H-NMR, IR spectroscopy and FAB-Mass spectrometry.

The structures of [MoTp*(O)Cl](μ-O)[MoTp*(Cl)(≡NC$_6$H$_4$X)], (p-X = Br) and [MoTp*(O)Cl](μ-O)[MoTp*(Cl)(≡NC$_6$H$_4$Y)], (m-Y = I, F) have been characterised by X-Ray diffaction method.

ÖZ

Bu çalışmada, [MoTp*(O)Cl$_2$]   [Tp* =Tris-(3, 5-dimetil-pirazol)borat] bileşiğinin toluen çözeltisinde p- ve m- anilin ligandlarıyla reaksiyonları incelenmiştir. Oluşan yeni binükleer oxo köprülü imido molybden (V) komplekslerinin [MoTp*(O)Cl](μ-O)[MoTp*(Cl)(≡NC$_6$H$_4$X)], (X = Cl, Br) and [MoTp*(O)Cl](μ-O) [MoTp*(Cl)(≡NC$_6$H$_4$Y)], (Y = I, F) ^{1}H-NMR, IR spektroskopisi ve kütle spektrometri yöntemleri ile yapıları aydınlatılmıştır.

[MoTp*(O)Cl](μ-O)[MoTp*(Cl)(≡NC$_6$H$_4$X)], (p-X = Br) ve [MoTp*(O)Cl] (μ-O)[MoTp*(Cl)(≡NC$_6$H$_4$Y)], (m-Y = I, F) bileşiklerin yapıları X-ray difraksiyon yöntemi ile de çözülmüştür.

TABLE OF CONTENS

LIST OF FIGURES

LIST OF TABLES

LIST OF SCHEMES

ABBREVIATIONS AND SYMBOLS

Tp : Trispyrazolylborate

Cp : Cyclopentadienyl

Tp*: Tris-(3,5-dimethyl-pyrazol)borato

Cp* : Pentamethylcyclopentadienyl

Tp^{pr} : Hydrotris-(3-isopropylpyrazolyl)borate

IR : Infrared

NMR : Nuclear Magnetic Resonance

δ : Chemical Shift

FAB : Fast Atom Bombartment

Et_3N : Triethylamine

AgOCOMe : Silver acetete

Py : Pyridine (NC_5H_5)

CaH_2 : Calcium Hydride

KTp* : Potassium hydrotris(3,5-dimethyl-1-pyrazolyl)borate

tlc : Thin Layer Chromatography

Me : CH_3

CH_2Cl_2 : Dichloromethane

$bdtCl_2$: 3,6-dichloro-1,2-benzenedithiolate

p- : para

m- : meta

$H_2NC_6H_4X$: p- functionalized anilines

$H_2NC_6H_4Y$: m- functionalized anilines

M^+ : Molecular ion

Mol wt. : Molecular weight

Chapter 1

INTRODUCTION

The work described in this thesis is concerned with oxo molybdenum trispyrazolylborate chemistry. In this chapter, some background information on this field is presented.

1.1. Oxo Molybdenum Trispyrazolylborate Chemistry

1.1.1. The Polypyrazolylborates

The polypyrazolylborate ligands $[BR_n(Pz)_{4-n}]^-$ were first synthesized by Trofimenko in 1966 [1], and the coordination chemistry of these ligands has been, and still is a vigorous research area [2]. Their synthesis is easily accomplished by the reaction of pyrazole or a substituted pyrazole with an alkali metal borohydride (Figure 1.1.).

In all these uninegative species, the boron exists in a tetrahedral environment and coordination to a metal ion occurs via the nitrogen atoms in the 2-position in each pyrazolyl ring. Bispyrazolylborates are therefore bidentate, while trispyrazolylborates are tridentate and occupy three facial coordination sites in its metal complexes. The facial coordination to three sites of a metal ion, their uninegative charge and donation of six electrons to the metal has resulted in a comparison with the cyclopentadienyl anion as a ligand [3].
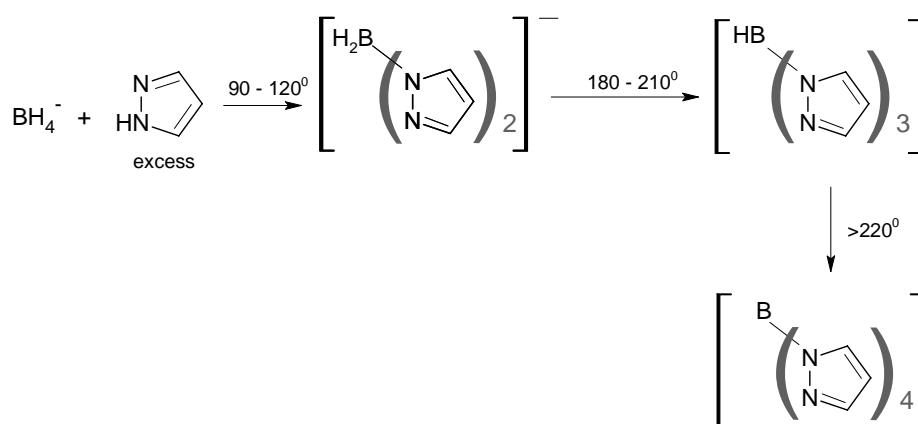
Figure 1.1. Prepration of polypyrazolylborates.

1.1.2. The Comparison of Tp and Cp Ligands

Tris(pyrazolyl)borate (Tp, $[HB(pz)_3]^-$), tris(3, 5-dimethyl-pyrazol)borato (Tp*, $[HB(3,5-Me_2pz)_3]^-$) (Figure1.2) can be compared to the ligands cyclopentadienyl (Cp, C_5H_5) and pentamethylcyclopentadienyl (Cp*, C_5Me_5) respectively [4], in that they are monoanionic, formally six electron donors which can occupy three facial coordination sites on a metal ion.

However there are some important differences. Firstly, the trispyrazolylborates are tripodal with C_{3v} symmetry, whereas the cyclopentadienyl ligands are pentagonal with D_{5h} [5]. Secondly, the Tp ligands act as strong σ-donor and weak π-acceptors in contrast to the Cp ligands which act as π-donors and π-acceptors [6].

Trispyrazolylborates are better donors and comparable acceptors than cyclopentadienyl.
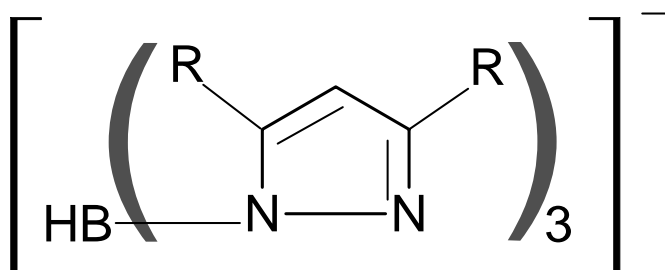
Figure 1.2. Hydrotris(1-pyrazolyl)borate ion (Tp : R = H), (**Tp* :** R = Me**).**

Molybdenum trispyrazolylborates are mainly six coordinate in contrast to the predominately seven coordinate species found in the analogous molybdenum-cyclopentadienyl chemistry. This is partially due to the steric effects of trispyrazolylborates, but also to the electronic influences of these ligands. The highly directional σ-orbitals on the nitrogens help to hybridise the metal into an octahedrally coordinate structure. The highly diffuse π-orbitals of cyclopentadienyl have no such influence on the metal [7].
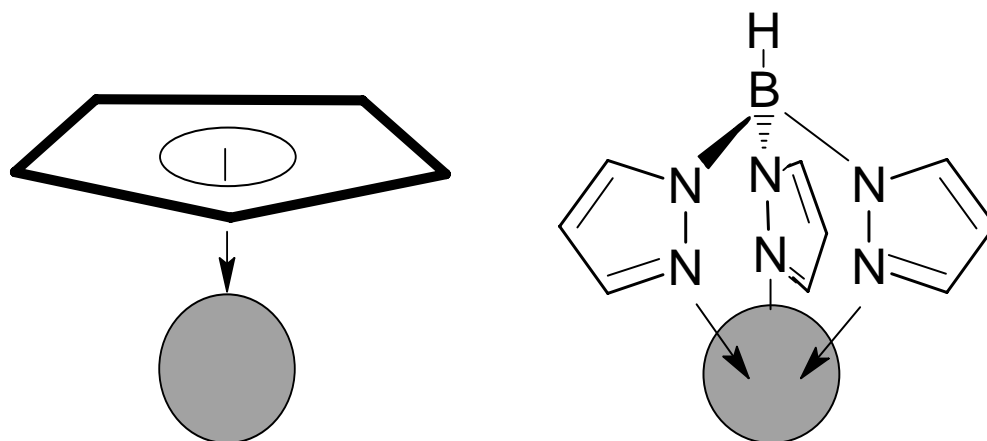
Figure 1.3. Comparison of trispyrazolylborate and cyclopentadienyl ligand coordination.

There is evidence to show that the trispyrazolylborate ligand forms stronger bonds to metals than cyclopentadienyl. Combined with the extra steric protection afforded this means that metal complexes of the trispyrazolylborate anions are genarally more thermodinamically stable. Thus stable trispyrazolylborate complexes have become more abundant than their counterparts containing cyclopentadienyl [8, 9].

The Tp* is an extremly bulky ligand and the methyl group in the 3-position help to envelop the metal in its coordination compounds. This can be seen from the Talmon cone angles for trispyrazolylborate, tris(3,5-dimethyl-pyrazol)borato, cyclopentadienyl and pentamethylcyclopentadienyl ligands which are 180°, 225°, 136° and 165°, respectively.

It is the steric and electronic properties of this tris(3,5-dimethyl-pyrazol)borato ligand that brings about stabilisation of formally coordinatively unsaturated complexes or, in many cases compounds which are otherwise air and moisture sensitive.

Cone angle = 180°
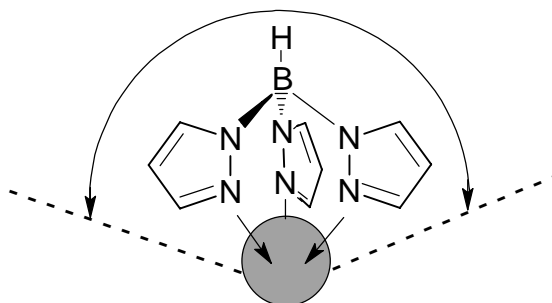
Cone angle = 225°
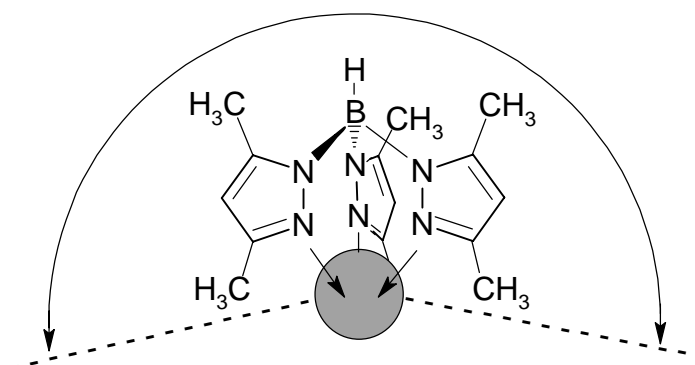
Figure 1.4. Comparison of trispyrazolylborate and tris(3,5-dimethyl-pyrazol)borato showing cone angles.

1.2. Oxo Molybdenum Compounds

1.2.1. Monomers

[MoTp*(O)Cl$_2$] (**1**) was obtained, a number of years ago, by Trofimenko by alumina treatment of the unchracterized red solution that be obtained from reaction of [MoTp*(CO)$_3$]⁻ (**2**) with thionyl chloride [10]. The red solution has since been chracterized as containing [MoTp*Cl$_3$] (**3**), [11] and it was found that the oxidation of this compound with dioxygen gave a good yield of the yellow-green crystalline complex [MoTp*(O)Cl$_2$] (**1**), [MoTp(O)Cl$_2$] (**4**) was made in an analogous manner. These monomers are paramagnetic, as expected for a d^1 system.
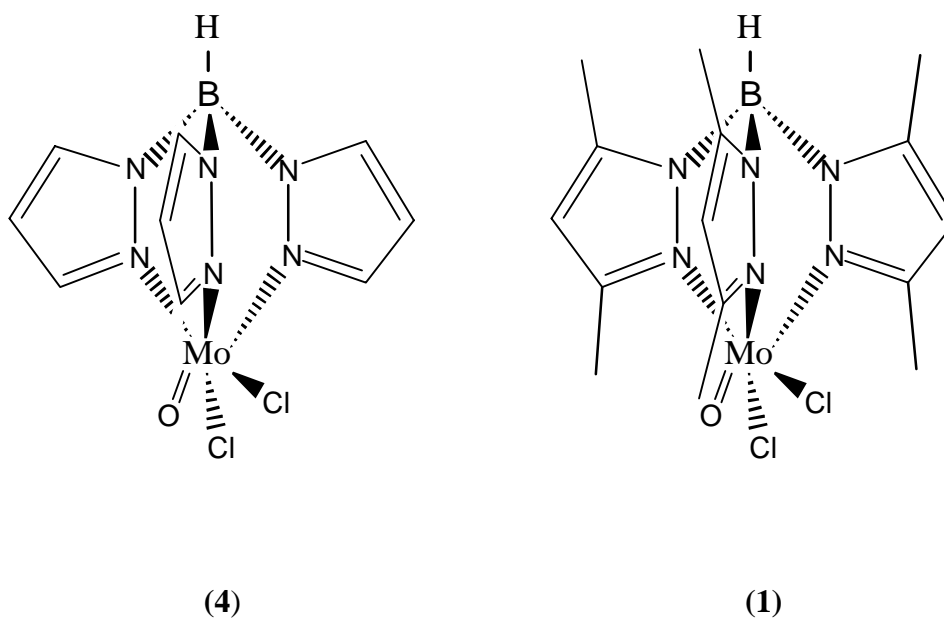
Figure 1.5. The structures of [MoTp(O)Cl₂], (4) and [MoTp*(O)Cl₂], (1).

The X-ray crystal structure of the complex [MoTp(O)Cl₂] is shown in Figure 1.6.
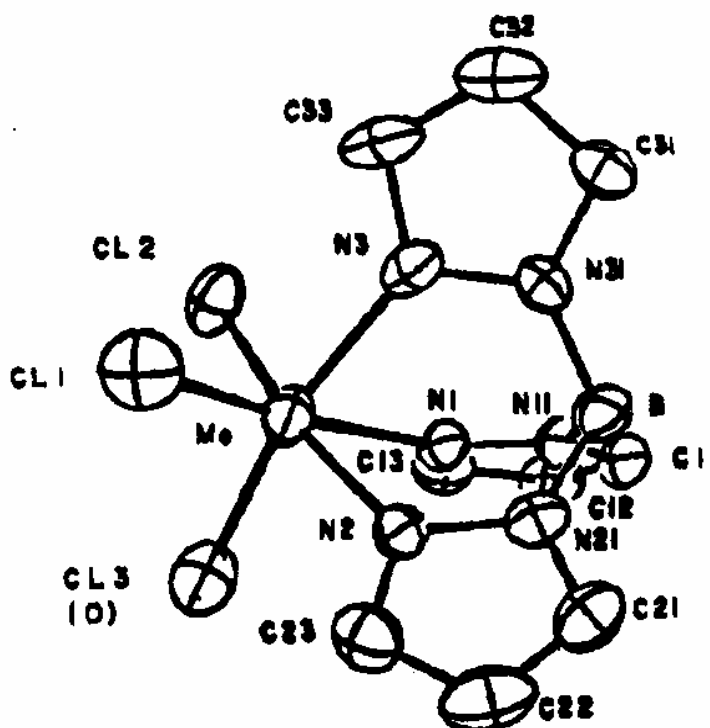
Figure 1.6. The crystal structure of [MoTp(O)Cl₂], (4).

1.2.2. Dimers

[Mo$_2$O$_4$(Tp)$_2$] (**5**), [12] was the major product obtained from the reaction of KHB(pz)$_3$ with solutions of [Mo(O)Cl$_5$]$^{2-}$ in aquoeous HCl solution (pH=2) according to a modification of a synthetic procedure developed by Melby for similar Mo$_2$O$_4^{2+}$ complexes [13].
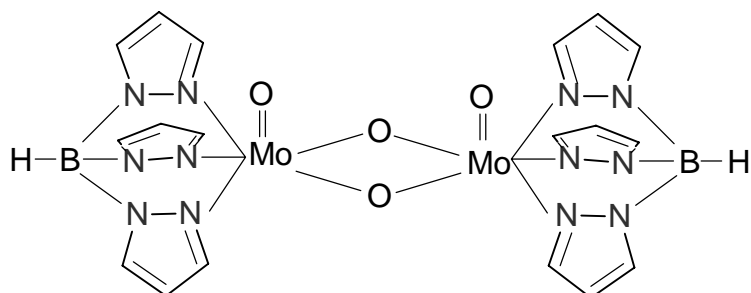
Figure 1.7. The structure of [Mo$_2$O$_4$(Tp)$_2$], (5).

Compound [Mo$_2$O$_4$(Tp)$_2$] (**5**) was reported [12] to be converted to the mono μ-oxo bridged species [MoTp(O)Cl]$_2$(μ-O) (**6**) with HCl (Scheme 1.1.), which was a chracteristic reaction of Mo$_2$O$_4^{2+}$ complexes[14].
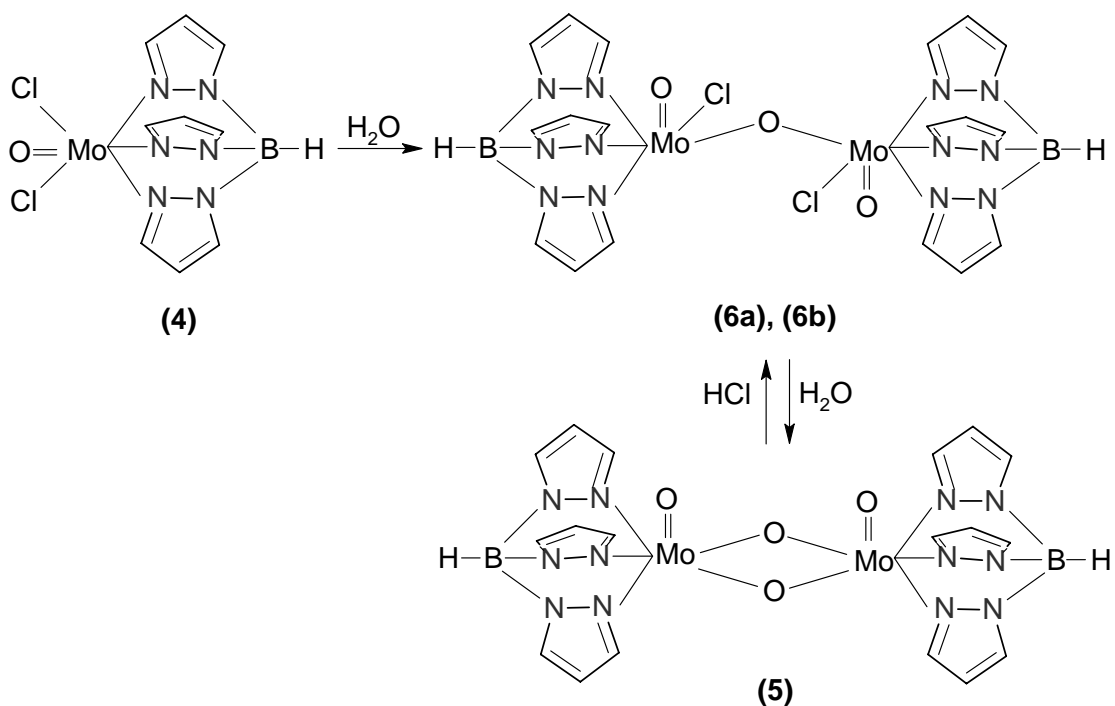
Scheme 1.1. Synthesis of polypyrazolylborate Mo (V) complexes.

Hydrolysis of the Mo(V) complex [MoTp(O)Cl$_2$], (4) leads to two geometrical isomers of formula [MoTp(O)Cl$_2$](μ-O), (6) (cis isomer (6a), 10 % yield) and (trans isomer (6b), % 60 yield), (Scheme 1.1.) [12].

The X-ray structures of (6a) and (6b) were determined [12].
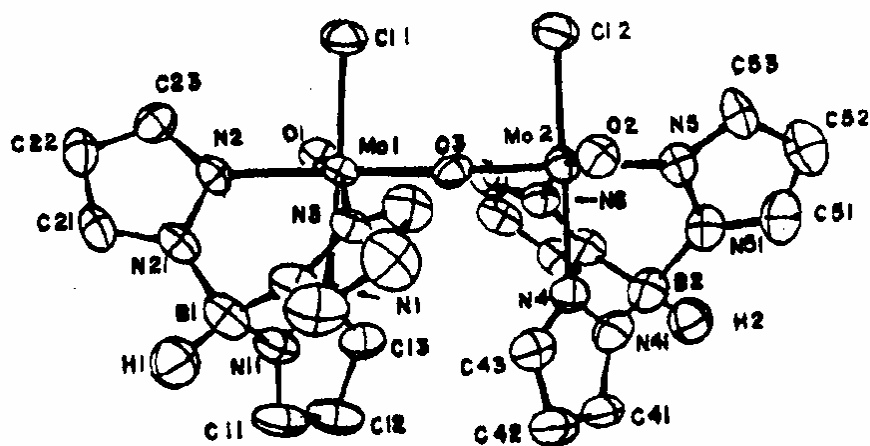
(cis isomer)
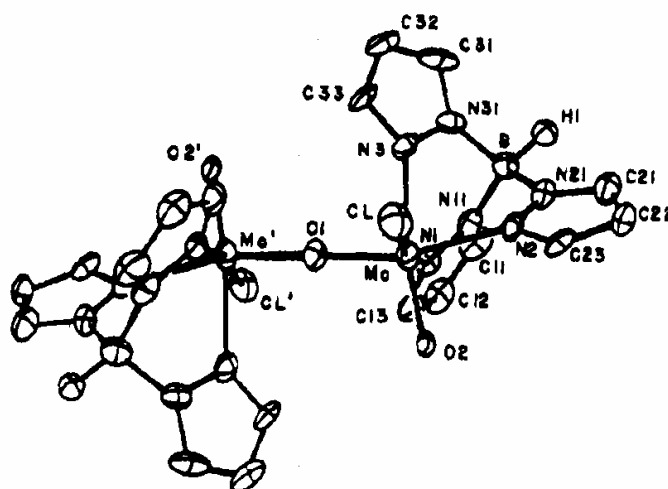
(trans isomer)

Figure 1.8. The crystal structures of (6a) and (6b).

Crystal structures showed them to be linear μ-oxo bridged Mo-O-Mo complexes. A deteailed FTIR and Raman experiments have been carried out related to symmetry dependence of bands associated with the Mo-O-Mo bridge [15].

7

McCleverty et al.have prepared [MoTp*(O)Cl$_2$](μ-O), **(7)** in good yield by the reaction of [MoTp*(O$_2$)Cl] **(8)** [16] with Ph$_3$P in wet toluene containing approximately 0.03 % water. Its crystal structure is shown in Figure 1.9.
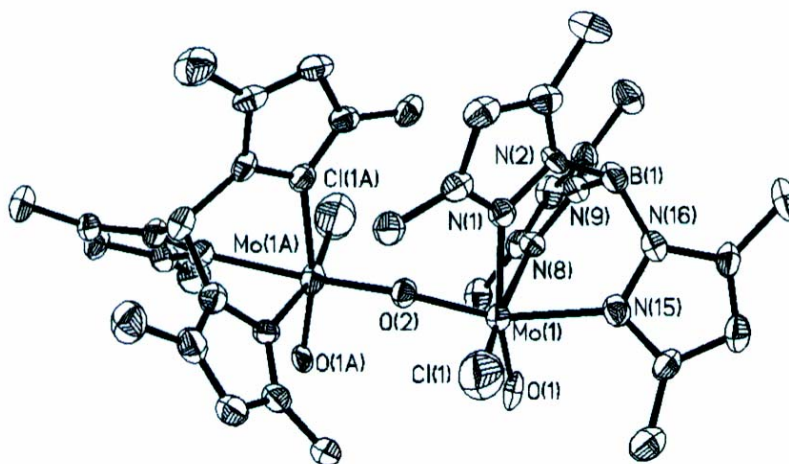
Figure 1.9. The crystal structure of [MoTp*(O)Cl$_2$](μ-O), (7).

1.2.3. Mixed-Valance Molybdenum (μ-O) Compounds

It was reported [17] that reaction of [MoTp*(O$_2$)Cl] **(8)** with the grignard reagent MeMgCl, MeMgI, or PhCHMgBr in tetrahydrofuran at –78 or – 42°C produced a deep brown reaction mixture after rapid disappearance of an initial transient green coloration to yield orange-brown [Mo$^{(V)}$Tp*(O)Cl(μ-O)Mo$^{(VI)}$Tp*(O$_2$)] **(9)**. The infrared, electronic spectroscopy and X-ray diffraction structure of **(9)** were reported.
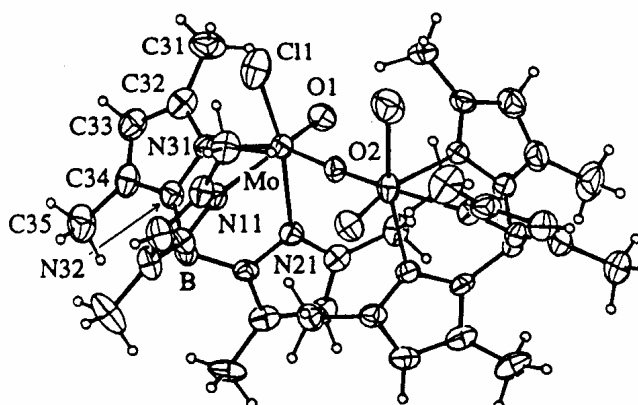
Figure 1.10. The crystal structure of [Mo$^{(V)}$Tp*(O)Cl(μ-O)Mo$^{(VI)}$Tp*(O$_2$)] (9).

1.2.4. Reactions of [MoTp*(O)Cl$_2$]

As it was mentioned before, [MoTp*(O)Cl$_2$] (**1**) complex was prepared by Trofimenko [10] as a product of the reaction of [MoTp*(CO)$_3$]$^-$ (**2**) with SOCl$_2$. [MoTp*(O)Cl]$^+$ fragment is very attractive to work with, because: (i) it is electronically simple (d^1), (ii) it is redox active and paramagnetic, (iii) it is synthetically easy to use, and (iv) the coordination chemistry and bioinorganic chemistry of oxo-molybdenum (V) complexes is general have been extensively studied, so their spectroscopic properties are fairly thoroughly understood [19].

Enemark and his cowerkers have developed a more convenient prepration for [MoTp*(O)Cl$_2$] [18]. Reaction of MoCl$_5$ with THF under anaerobic conditions (equation 1) yields the intermediate part [Mo(THF)$_2$(O)Cl$_3$] first, by abstraction of an oxygen atom from the solvent. Addition of KTp* to the reaction mixture yield 16 e$^-$ [MoTp*(O)Cl$_2$] (**1**) complex.

$$MoCl_5 \xrightarrow{\text{THF}} MoOCl_3(THF)_2 \xrightarrow{\text{KTp*}} MoTp^*(O)Cl_2$$

(equation 1)
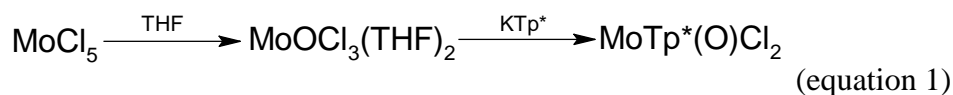
Enemark et al. have first prepared a series of mononuclear oxo molybdenum (IV), (V) complexes [MoTp*(O)Cl(X)], (X = OR, SR, py, NCS etc.; R=Ph, Alkyl; py = NC$_5$H$_5$ (**10**)) by dissociation of chloride and subsequent coordination of the new ligand and determined their electrochemical and spectroscopic properties.
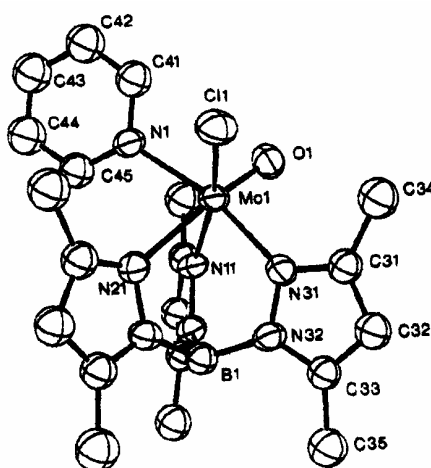
(**10**)
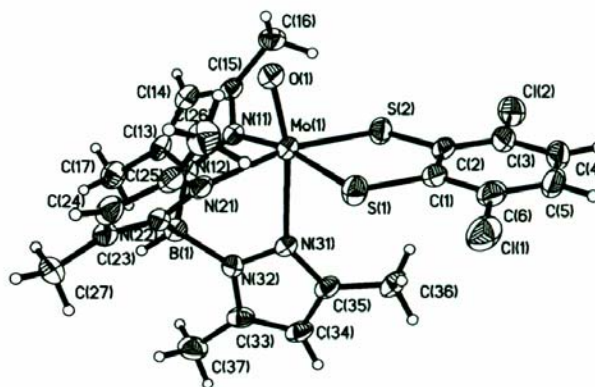
(11)

Figure 1.11. The crystal structure of [MoTp*(O)Cl(NC$_5$H$_5$)], (10) and [MoTp*(O)Cl(bdtCl$_2$)], (11) (bdtCl$_2$ = 3,6-dichloro-1,2-benzenedithiolate).

Mccleverty et al. reported the mononuclear compounds [MoTp*(O)Cl(=NR)] **(12)** (R= 4-tolyl **(12a)** and C$_6$H$_4$NMe$_2$-4 **(12b)**, C$_6$H$_4$NH$_2$-4 **(12c)**) and the dinuclear complex [MoTp*(O)Cl]$_2$(NC$_6$H$_4$N) **(13)** by the reaction of oxo-molybdenum (V) precursor [MoTp*(O)Cl$_2$] (1) with arylamines RNH$_2$. These preprations were reported as a new route into oxo imido Mo(VI) chemistry apart from a single previous example [20].
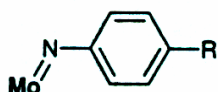
R= 4-tolyl **(12a)**

R= C$_6$H$_4$NMe$_2$-4 **(12b)**

R= C$_6$H$_4$NH$_2$-4 **(12c)**
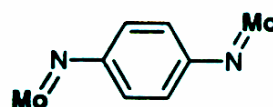
(13)
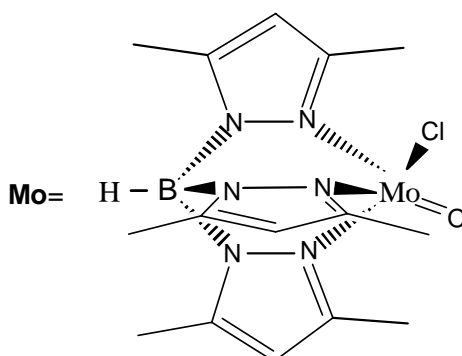
Figure 1.12. The structures of complexes (12a), (12b), (12c), (13).

McCleverty et al. have prepared a series of dinuclear complexes [MoTp*(O)Cl] (μ-OO), where ''OO'' represents one of the series of diphenolate bridging ligands [1,4-O(C_6H_4)$_n$O]$^{2-}$ (n=1-4), ((**14**) for n=1) or [1,3-OC$_6$H$_4$O]$^{2-}$ (**15**). The complexes contain two paramagnetic (d^1), redox active metal centers [21].
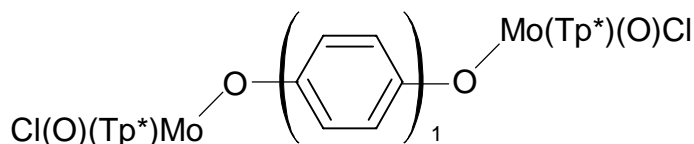
(14)
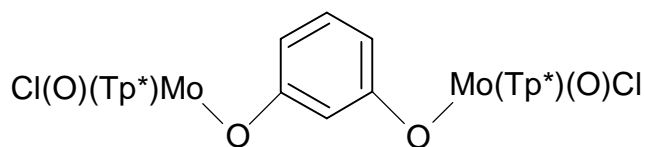
(15)

Figure 1.13. The structural formulas of complexes containing diphenolate bridging ligands.
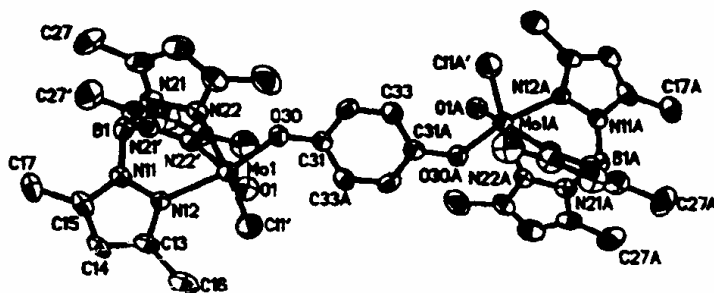
(14)
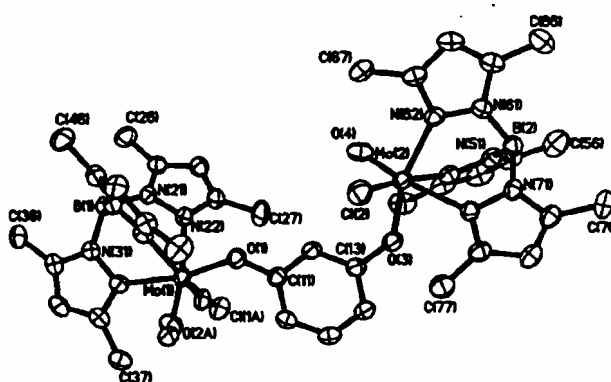
(15)

Figure 1.14. The crystlal structures of the complexes (14) and (15).

11

The trinuclear complexes [MoTp*(O)Cl](μ-1, n-$C_6H_4O_2$)[MoTp*(O)] (μ-1, n-$C_6H_4O_2$)[MoTp*(O)Cl], (n=3, 4) have been prepared by McCleverty et al. [22], in which a chain of three paramagnetic oxo-Mo(V) fragments are linked by two 1, 4-[OC_6H_4O]$^{2-}$ (n=4) (16) (Scheme 1.2.) or 1, 3-[OC_6H_4O]$^{2-}$ (n=3) (17) bridging ligands.
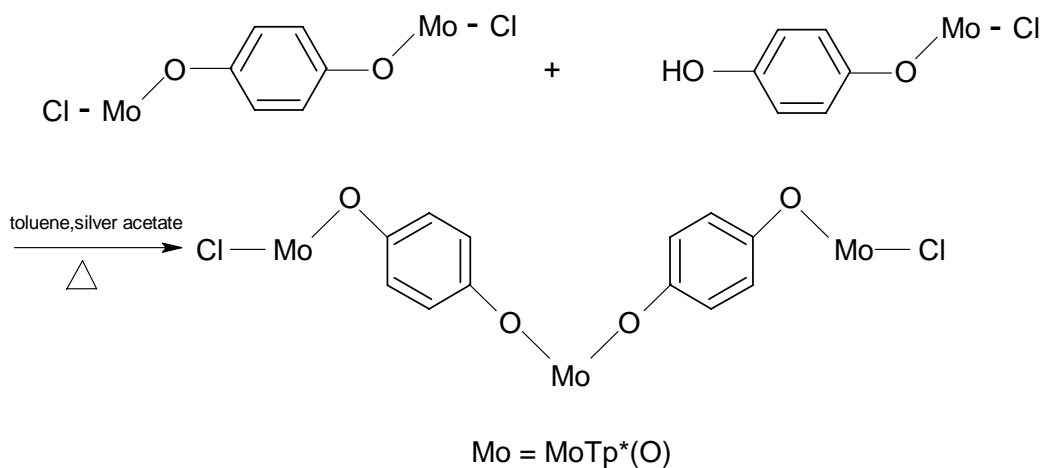
Scheme 1.2. Synthesis of complex (16).
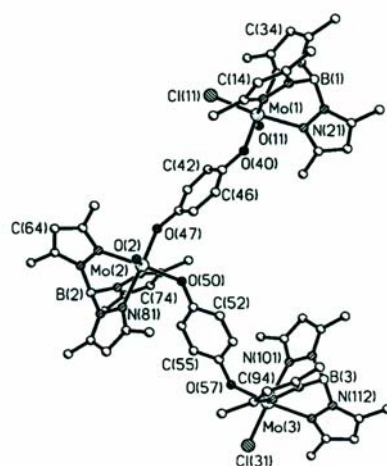
Figure 1.15. The crystal structure of [MoTp*(O)Cl](μ-1, 4-$C_6H_4O_2$) [MoTp*(O)] (μ-1, 4-$C_6H_4O_2$)[MoTp*(O)Cl] (16).

Chapter 2

EXPERIMENTAL STUDY

2.1. Experimental Techniques for Handling Air-Sensitive Compounds

All compouds synthesized in this study are air and moisture sensitive during the reactions. Although sythesizing air sensitive compounds may at first appear difficult, under proper precaution and with appropriate manipulation tool and techniques, they may be sythesized as easily as ordinary compounds [23]. For carrying out experiments with exclusion of air the falowing techniques are employed.

1) Vacuum-Line Technique
2) Schlenk Technique

2.2. The Vacuum-Line Technique

2.2.1. The Double Manifold

If you wish to carry out reactions under dry and inert conditions, a double manifold is an extremly useful piece of apparatus (Figure 2.1.).
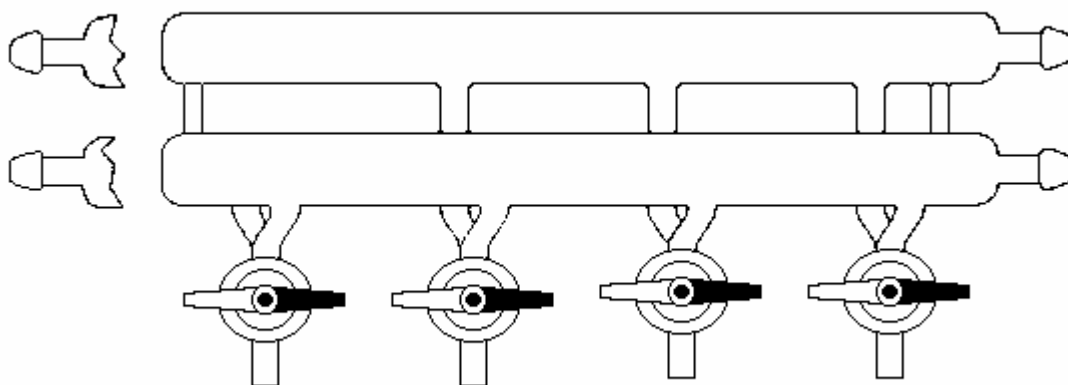
Figure 2.1. The double manifold.

The manifold consists of two glass barrel. One barrel of the manifold is connected to a high vacuum pump another to dry inert gas (Figure 2.2.). Thus, at the turn of the tap, equipment connected to the manifold can be alternately evacuated or filled with inert gas.
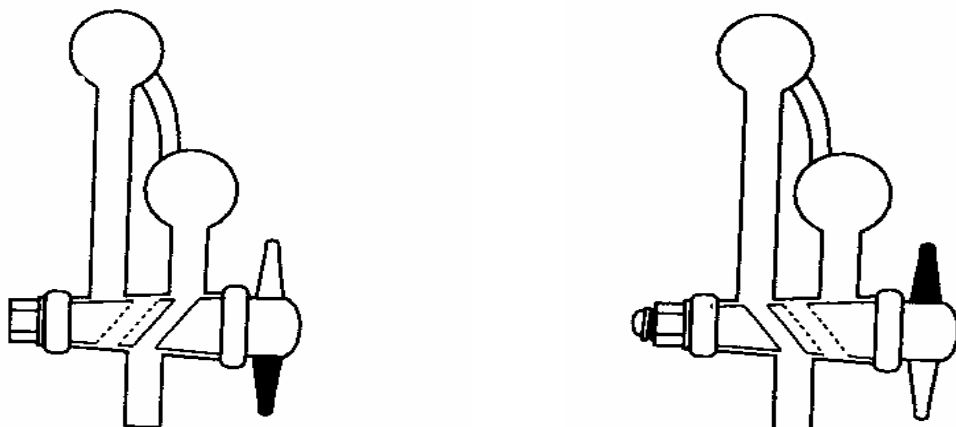
(a) Tap switched to vacuum　　　　　　**(b) Tap switched to inert gas**

Figure 2.2. Cross section through a double oblique tap.

2.2.2.The Schlenk Technique

To use a schlenk glassware provides facility during the reactions under N_2, with the schlenk tube one can transfer a solid or liquid in an atmosphere of an inert gas, such as nitrogen or argon [24, 25].

The basic and simplest schlenk tube is shown in Figure 3.3.The schlenk tube is stoppered and evacuated by pumping through D.By introducing the inert gas through A the tube is filled with the inert gas. The tap is turned through 90° to let gas pass through the tail part and then is turned through 90° to allow gas into the flask.
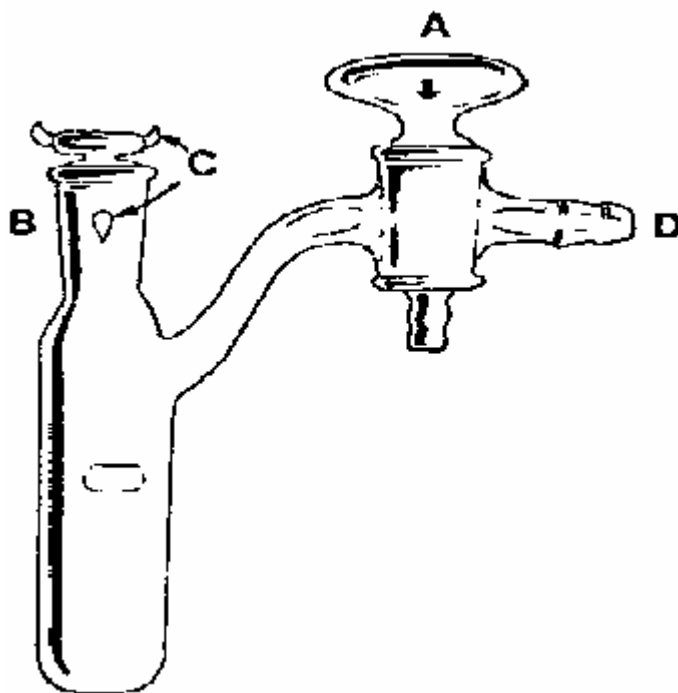
Figure 2.3. The schlenk tube.

2.3. Purification of Solvents

The solvents used are purified, dried under nitrogen by distillation system. A solvent still is used for this purpose [26, 27]. This system provides removing the small amount of impurities and any water from the solvent. An example of a solvent still is shown in Figure 2.4.

It consist of a large distillation flask, connected to a reflux condenser via a piece of glassware which can simply be a pressure equalizing funnel modified by the inclusion of a second stopcock. Since the production of very dry solvents usually requires the exclusion of air from the apparatus, the still is fitted so that it can be operated under an inert atmosphere . Firstly, drying agent and solvent are added to the distillation flask under N_2. With the stopcock A open, the solvent simply refluxes over the drying agent. When the stopcock A is closed, the solvent vapor passes up the narrow tube and dry solvent collects in the central piece of the apparatus. When the required volume of the solvent has been collected, it can be run off through the stopcock B. The solvents were prepared for the use as described below.

Toluene: The solvent was refluxed over CaH_2 and then distilled and stored over 4A° molecular sieves.

Dichloromethane: The same procedure was used in purification of toluene.

Hexane: The same procedure was used in purification of toluene.
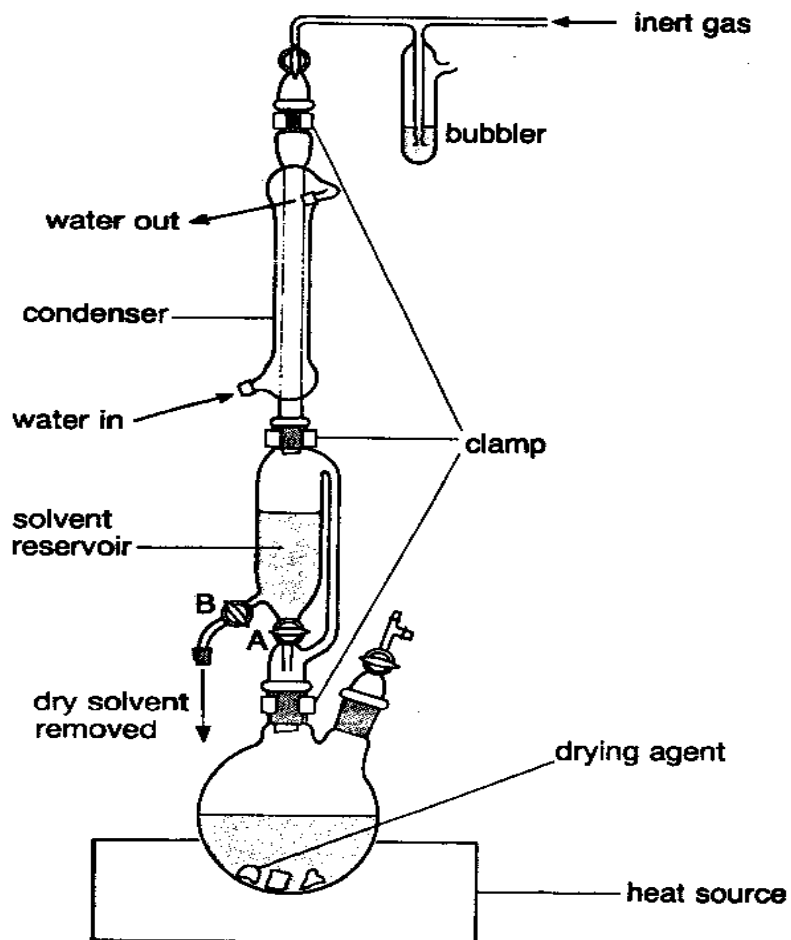
Figure 2.4. Solvent still.

2.4. Materials and Methotds

All preprations and manipulations were carried out with schlenk techniques under an oxygen free nitrogen atmosphere. All glassware was oven dried at 120 °C. Solvents were dried by standart procedures, distilled and kept under nitrogen over 4A° molecular sieves.

The starting materials [MoTp*(O)Cl$_2$] and KTp* were prepered according to the literature procedures [18] .

The products were characterized by IR, ^{1}H-NMR spectroscopy and FAB mass spectrometry. [MoTp*(O)Cl](μ-O)[MoTp*(Cl)($\equiv$NC$_6$H$_4$X)], (p-X = Br) and [MoTp*(O)Cl](μ-O)[MoTp*(Cl)($\equiv$NC$_6$H$_4$Y)], (m-Y = I, F) were characterised by X-ray diffaction study. Infrared spectra were recorded on a Magna IR spectrophotometer as pressed KBr disks. ^{1}H-NMR spectra were recorded in CDCl$_3$ on 400 MHz High Performance Digital f.t.-n.m.r. at TUBITAK. Mass spectra analyses were performed on Joel AX505 FAB device using Xe at 3KV positive ion matrix m-NBA (meta-nitrobenzyl alcohol). The crystal structure determinations were done by using a Bruker SMART CCD area-dedector diffractometer by Dr. J. C. Jeffery at Bristol University.

2.5. Syntheses

2.5.1. Prepration of [MoTp*(O)Cl](μ-O)[MoTp*(Cl)($\equiv$NC$_6$H$_4$F)], (I); (trans isomer) and [MoTp*(O)Cl](μ-O)MoTp*(Cl)($\equiv$NC$_6$H$_4$F)], (II); (cis isomer)

A mixture of [MoTp*(O)Cl$_2$] (0.4 g, 0.83 mmol), 3-floro aniline (0.18 g, 1.66 mmol) and dry Et$_3$N (0.6 cm^3) in dry toluene (20 cm^3) was heated to reflux with stirring under N$_2$ for 14 h. During which time the solution became dark red-brown in colour. The mixture was cooled, filtered and evaporated to dryness.The residue was dissolved in dichloromethane and chromatographed on silica gel using CH$_2$Cl$_2$/n-hexane (9:1, v/v) as eluant. Two red-brown fractions were collected , crystallised from CH$_2$Cl$_2$/n-hexane and identified, respectively, as [MoTp*(O)Cl](μ-O)[MoTp*(Cl)($\equiv$NC$_6$H$_4$F)], **(I)**; and [MoTp*(O)Cl](μ-O)MoTp*(Cl)($\equiv$NC$_6$H$_4$F)], **(II)**.

2.5.2. Preparation of [MoTp*(O)Cl](μ-O)[MoTp*(Cl)(≡NC$_6$H$_4$Br)], (III); (trans isomer) and [MoTp*(O)Cl](μ-O)MoTp*(Cl)(≡NC$_6$H$_4$Br)], (IV); (cis isomer)

A mixture of [MoTp*(O)Cl$_2$] (0.4 g, 0.83 mmol), 4-bromo aniline (0.28 g, 1.66 mmol) and dry Et$_3$N (0.6 cm^3) in dry toluene (20 cm^3) was heated to reflux with stirring under N$_2$ for 16 h. The reaction was fallowed by tlc using the procedure described above for (I) and (II) to give two dark-red bands identified as [MoTp*(O)Cl](μ-O) [MoTp*(Cl)(≡NC$_6$H$_4$Br)], **(III)**; and [MoTp*(O)Cl](μ-O)[MoTp*(Cl) (≡NC$_6$H$_4$Br)], **(IV)**.

2.5.3. Prepration of [MoTp*(O)Cl](μ-O)[MoTp*(Cl)(≡NC$_6$H$_4$Cl)], (V)

A mixture of [MoTp*(O)Cl$_2$] (0.4 g, 0.83 mmol), 4-chloro aniline (0.21 g, 1.64 mmol) and dry Et$_3$N (0.6 cm^3) in dry toluene (20 cm^3) was heated to reflux with stirring under N$_2$ for 16 h. The solvent was then removed in vacuoand the crude red solid was purified by column chromatography over silica gel using CH$_2$Cl$_2$/n-hexane (1:1, v/v) as eluant. The major claret-red band was collected, crystallised from CH$_2$Cl$_2$/n-hexane.

2.5.4. Prepration of [MoTp*(O)Cl](μ-O)[MoTp*(Cl)(≡NC$_6$H$_4$I)], (VI)

A mixture of [MoTp*(O)Cl$_2$] (0.4 g, 0.83 mmol), 3-Iodo aniline (0.36 g, 1.64 mmol) and dry Et$_3$N (0.6 cm^3) in dry toluene (20 cm^3) was heated to reflux with stirring under N$_2$ for 18 h. The mixture was then cooled and the solvent was removed in vacuo. The first dark-red solid was purified by column chromatography (silica, dichloromethane/n-hexane), (4:6, v/v) as eluant and recrystallised from dichloromethane/n-hexane to give a dark-red band identified as [MoTp*(O)Cl](μ-O) [MoTp*(Cl)(≡NC$_6$H$_4$I)].

Chapter 3

RESULTS AND DISCUSSION

Reaction of [MoTp*(O)Cl$_2$] (**1**),   [Tp* = Tris(3, 5-dimethyl-pyrazol)borato] p- and m- functionalized anilines, H$_2$NC$_6$H$_4$X and H$_2$NC$_6$H$_4$Y (p-X = Cl, Br; m-Y = I, F) (Figure 3.1.) in the presence of triethylamine in toluene produced binuclear oxo bridged imido molybdenum complexes [MoTp*(O)Cl](μ-O)[MoTp*(Cl)(≡NC$_6$H$_4$X)], (X = Cl, Br) and [MoTp*(O)Cl](μ-O)[MoTp*(Cl)(≡NC$_6$H$_4$Y)], (Y = I, F). The geometric isomers of (**I**) and (**III**) were also isolated and their structures were determined by X-ray diffraction method.

(X=Cl, Br)   (Y=F, I)

Figure 3.1. The structures of p- and m- functionalized anilines.
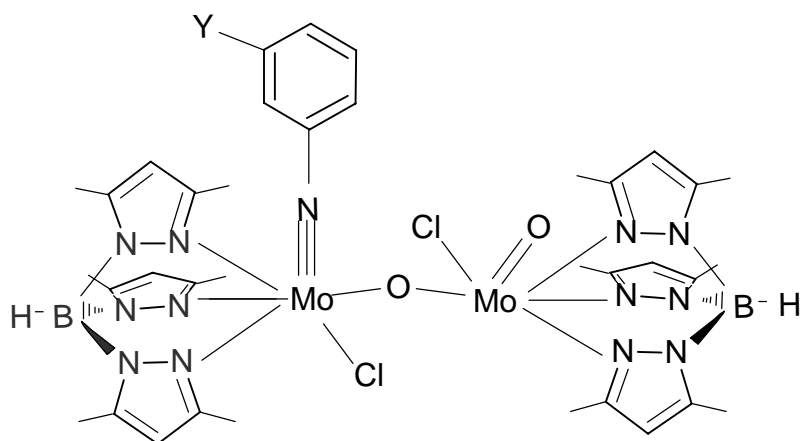
Figure 3.2. The structures for the complexes (I), **(VI)**.
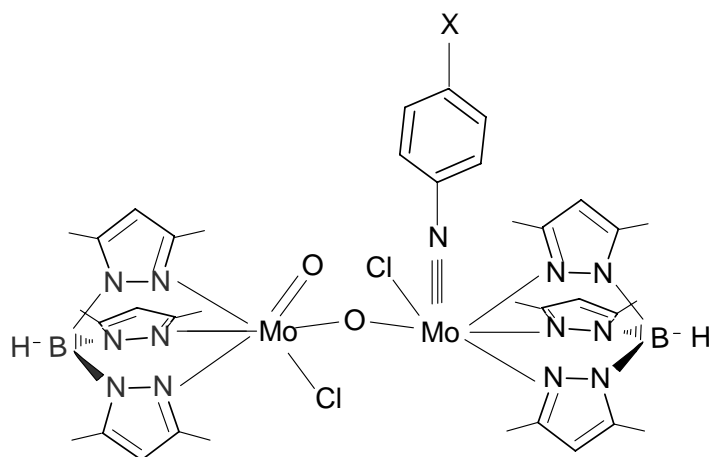
Figure 3.3. The structures for the complexes (III), (V).
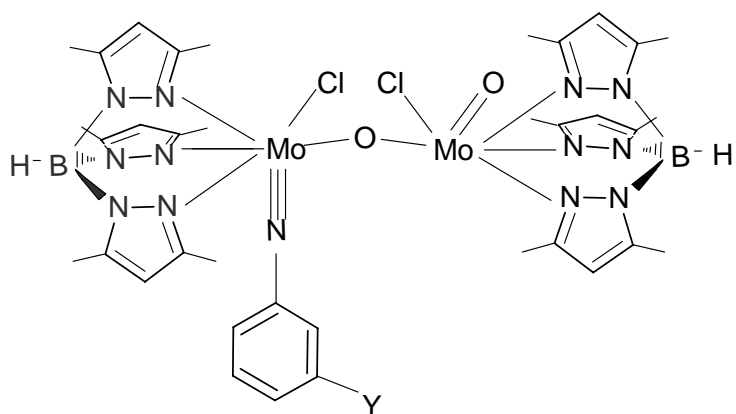
Figure 3.4. The structure for the complex (II).
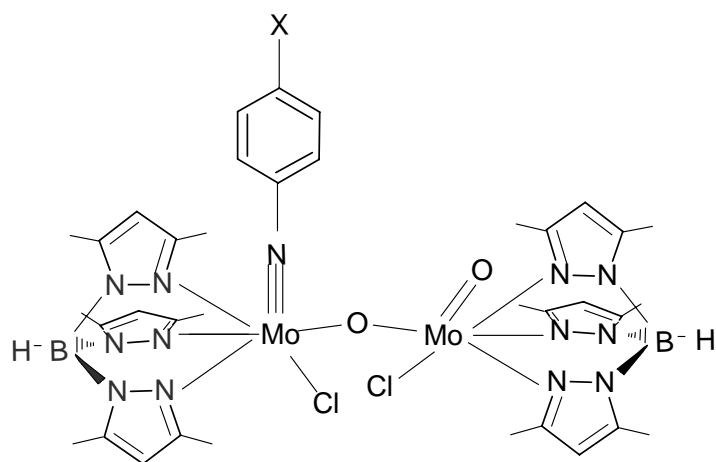
Figure 3.5. The structure for the complex (IV).

The reactions were performed at reflux temperature over periods ranging from 14-24 h. Formation of the complexes was fallowed by thin layer chromatography (tlc) using CH_2Cl_2/n-hexane (v:v, different ratios) as eluant. The products were readily purified by column chromatography on silica gel 60 (70-230 mesh) using the same solvent mixture as eluant. The complexes are air-stable and red in colour. They are soluble in chlorinated solvents.

3.1. Spectroscopic Studies

Mass spectrometric data were in accord with the structures obtained from X-ray diffraction analyses. Molecular ions and (M^+-Cl) were observed for all complexes (Table 3.1.). Their spectra are shown in Figure 3.6.-3.11. No general trend for the rest of the fragmentation in the molecules could be determined.

Table 3.1. Mass spectral data for [MoTp*(O)Cl](μ-O)[MoTp*(Cl) (≡NC$_6$H$_4$X)], (X = Cl, Br) and [MoTp*(O)Cl](μ-O)[MoTp*(Cl)(≡NC$_6$H$_4$Y)], (Y = I, F).

Compound	Mol wt.	M^+	M^+-(Cl)
(I)	998.2	998.2	964.3
(II)	998.2	998.1	962.1
(III)	1059.2	1059.1	1024.1
(IV)	1059.2	1059.1	1024.2
(V)	1014.7	1014.6	979.2
(VI)	1106.1	1104.9	1069.4
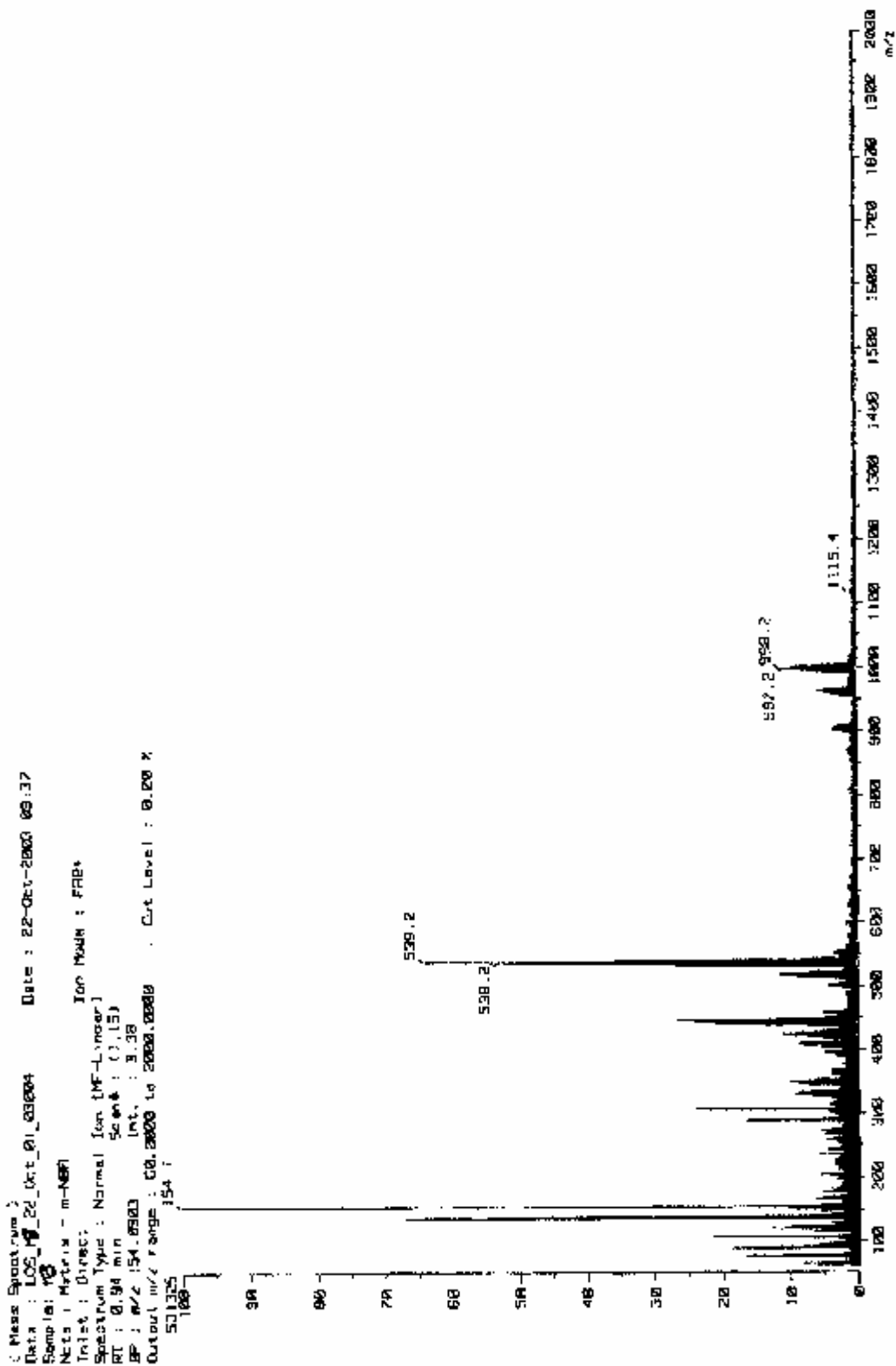
Figure 3.6. The FAB-Mass spectrum of [MoTp*(O)Cl](μ-O) [MoTp*(Cl)(≡NC₆H₄F)], (I).
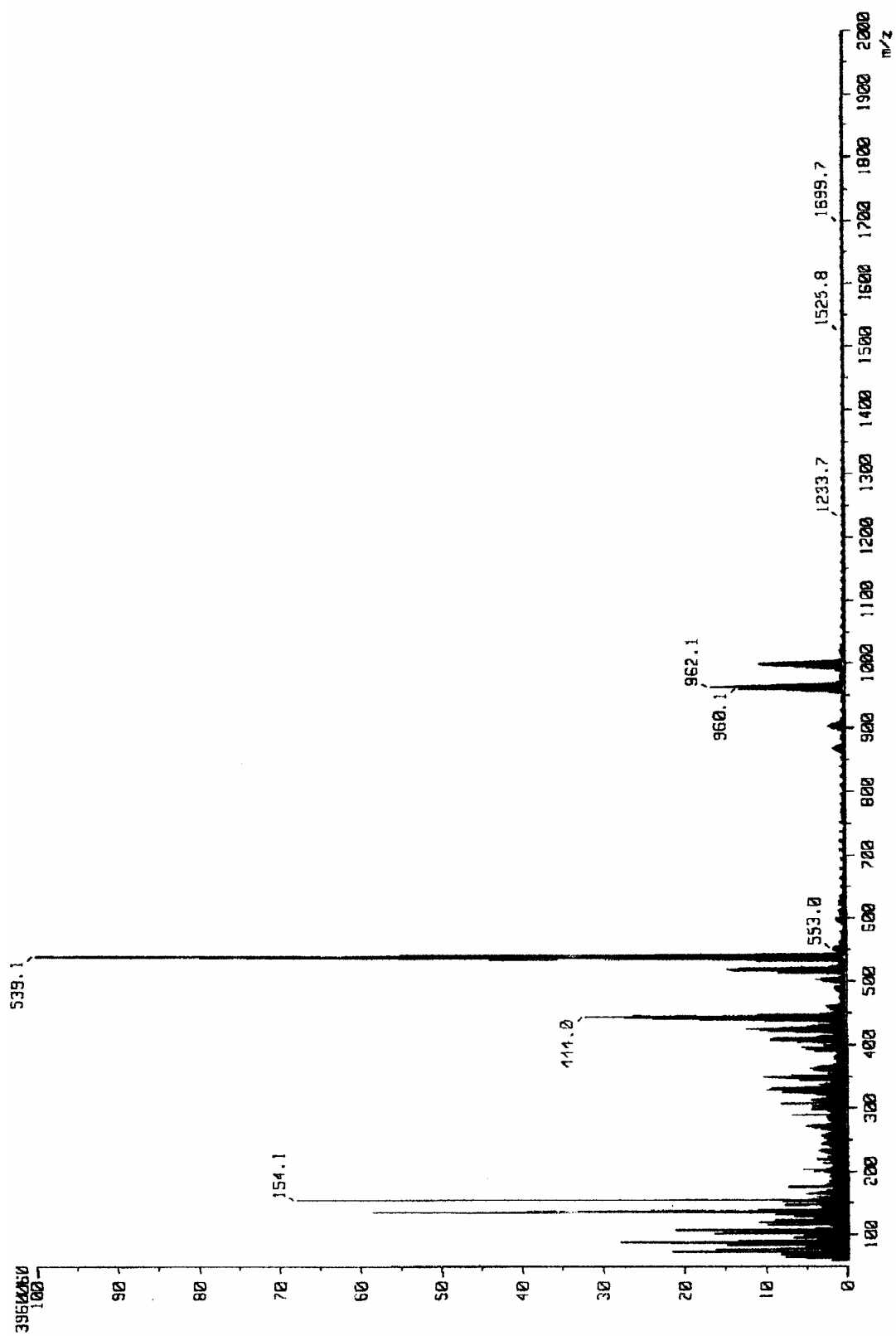
Figure 3.7. The FAB-Mass spectrum of [MoTp*(O)Cl](μ-O) [MoTp*(Cl)(≡NC₆H₄F)], (II).
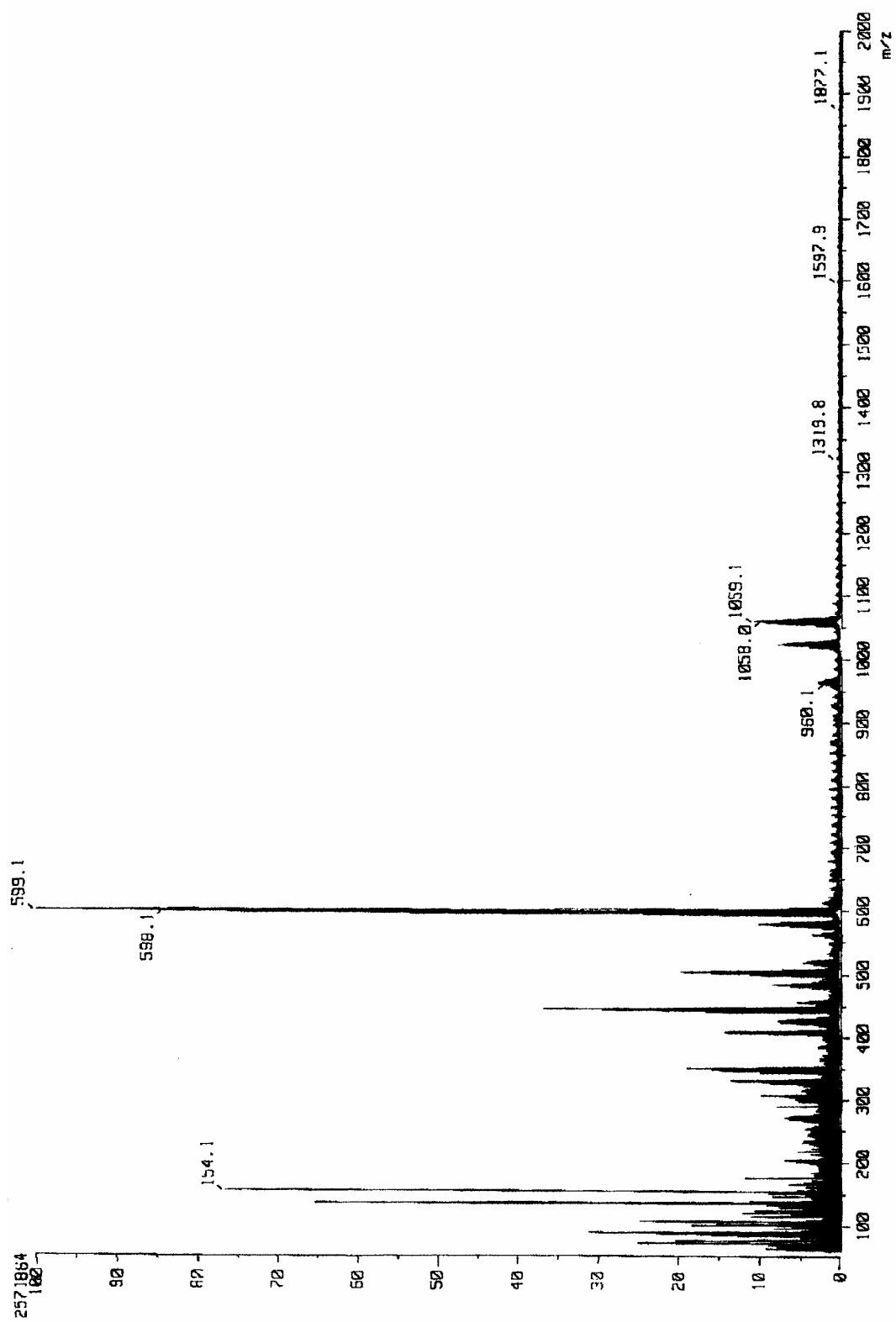
Figure 3.8. The FAB-Mass spectrum of [MoTp*(O)Cl](μ-O)[MoTp*(Cl)(≡NC₆H₄Br)],(III).
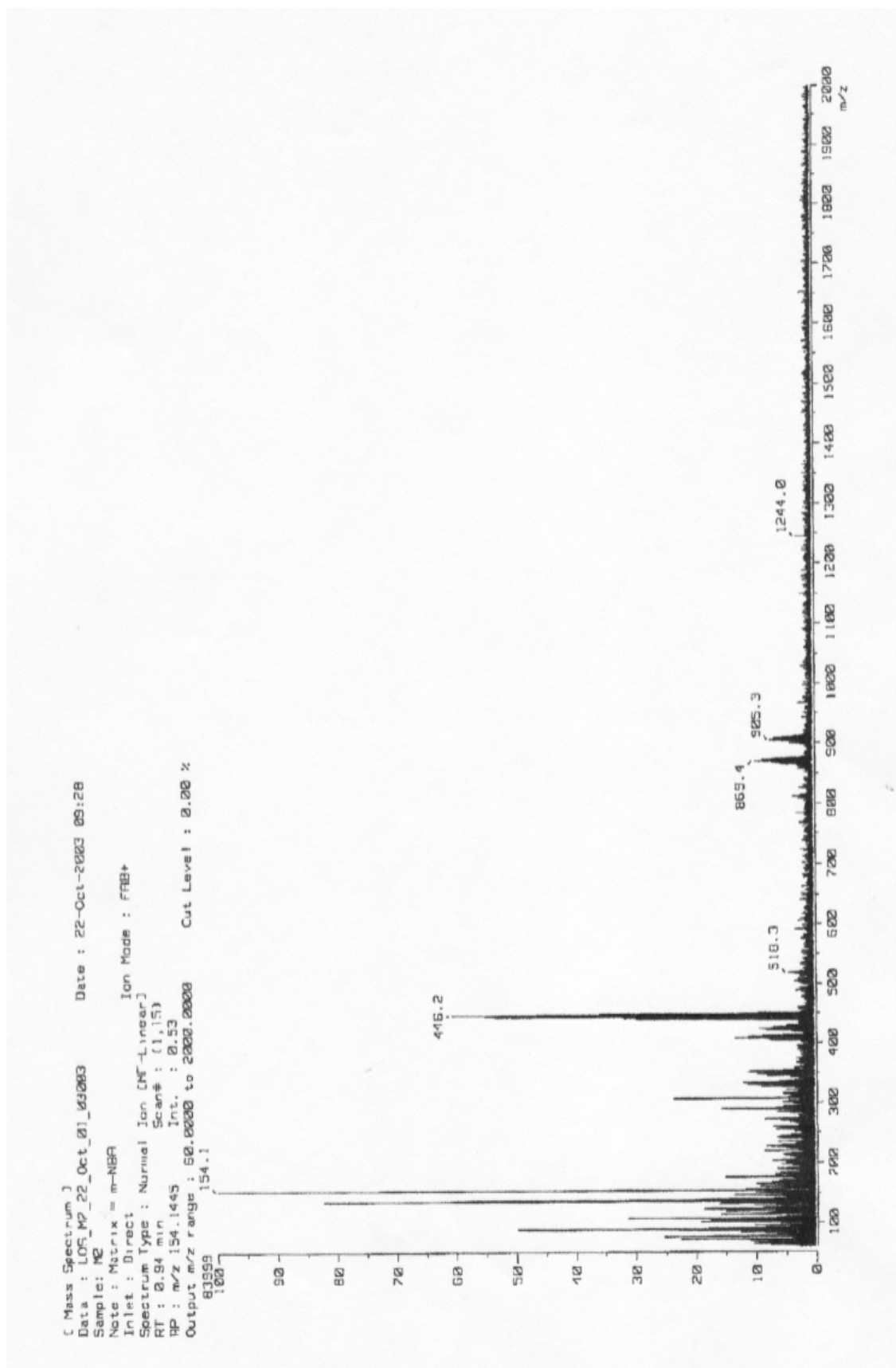
Figure 3.9. The FAB-Mass spectrum of [MoTp*(O)Cl](μ-O)[MoTp*(Cl)(≡NC₆H₄Br)],(IV).
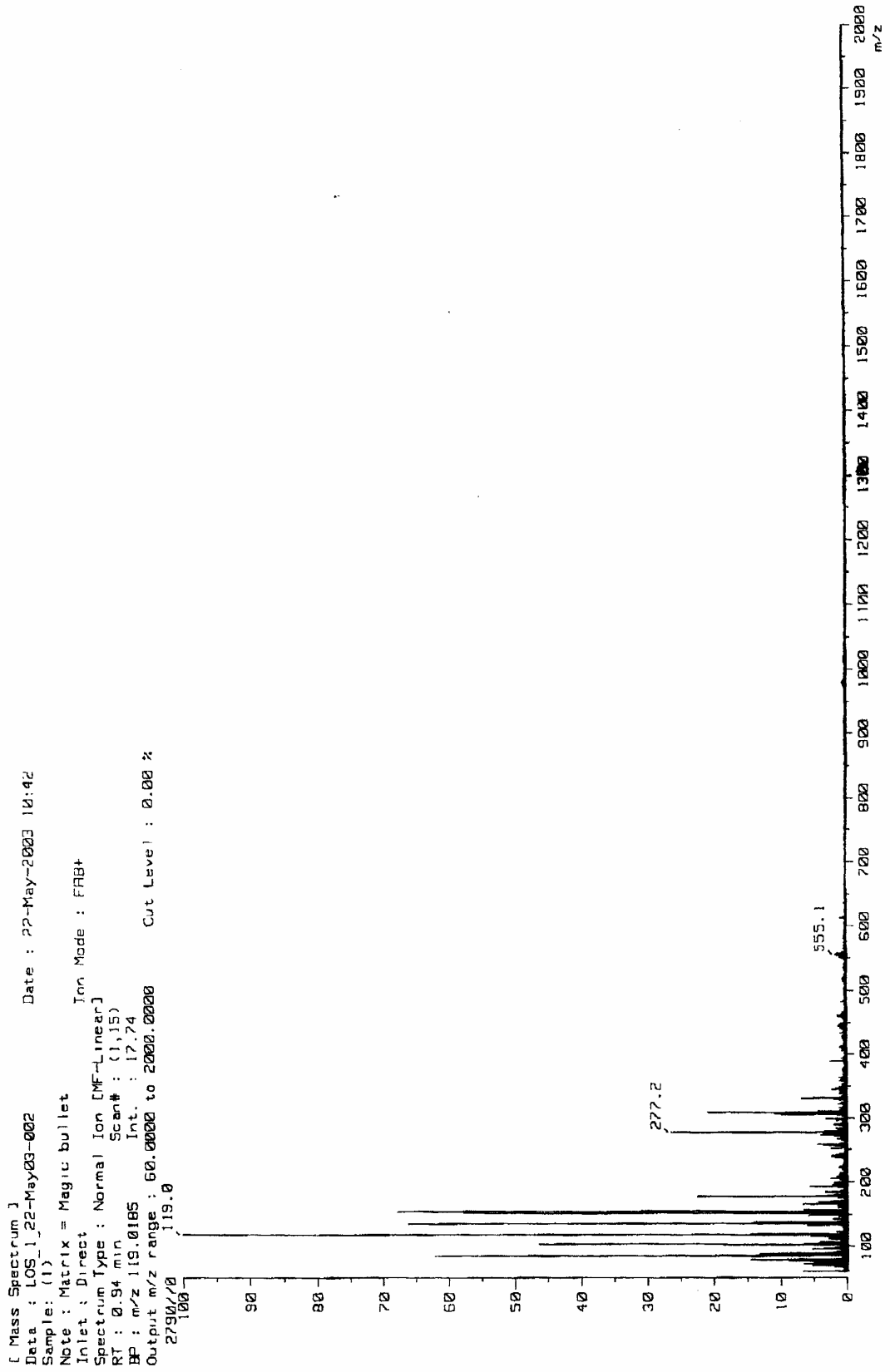
Figure 3.10. The FAB-Mass spectrum of [MoTp*(O)Cl](μ-O)[MoTp*(Cl)(≡NC₆H₄Cl)],(V).

26
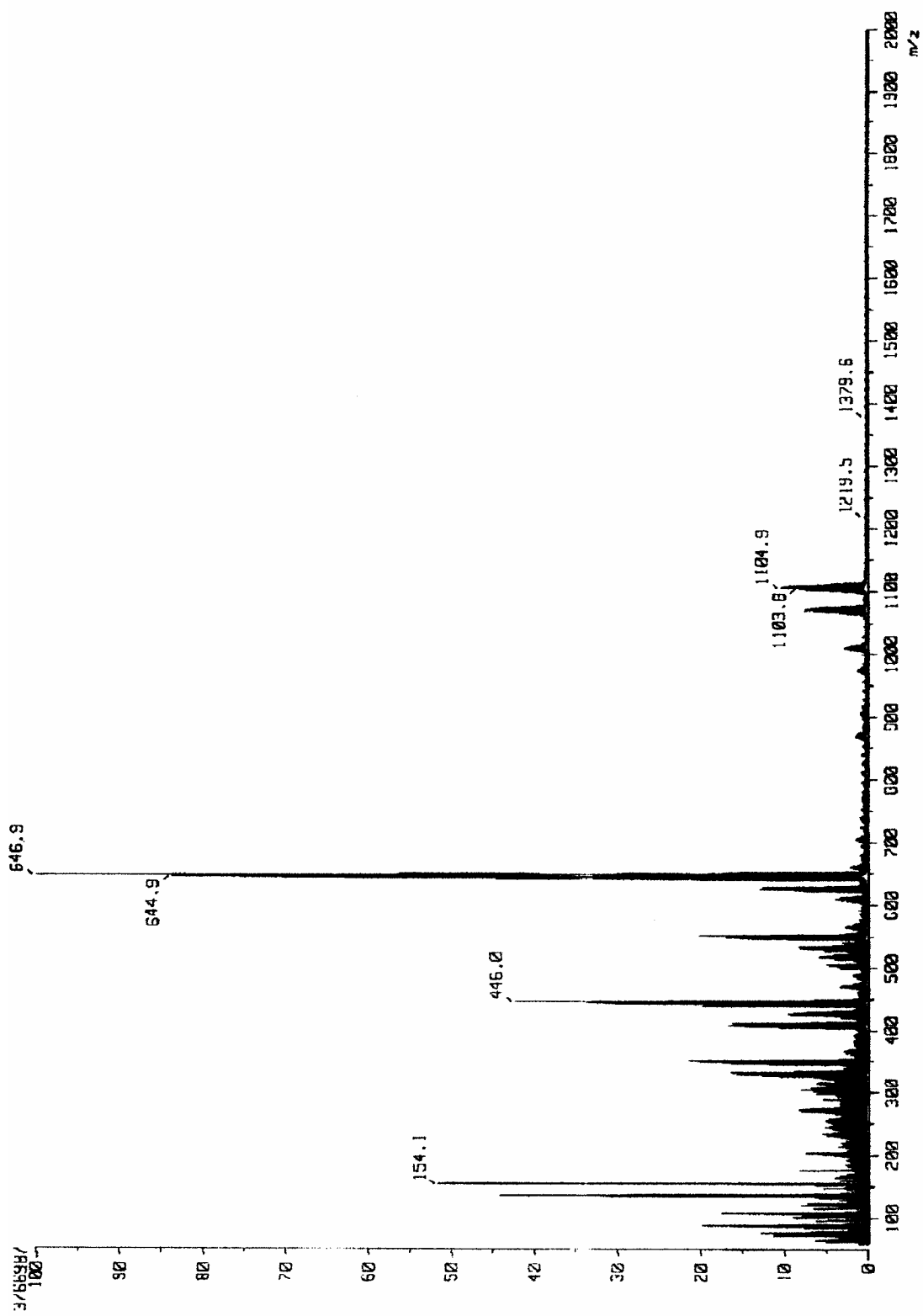
Figure 3.11. The FAB-Mass spectrum of [MoTp*(O)Cl](μ-O) [MoTp*(Cl)(≡NC₆H₄l)], (VI).

IR spectra data for the complexes **(I)-(VI)** are given in Table 3.2. and their spectra are shown in Figure 3.12-3.17. All complexes exhibit the expected absorptions due to the Tp* ligand (ca. 2500 cm^{-1} due to $\nu_{(BH)}$ and 1400 cm^{-1} associated with the pyrazolyl ring).

The IR spectra of compounds **(I)-(VI)** possess bands chracteristic of the terminal Mo=O unit (ca. 950 cm^{-1}). This value was reported at 964 cm^{-1} for the starting material [MoTp*(O)Cl$_2$] [18]. For the compounds [MoTp(O)Cl$_2$](μ-O), cis isomer **(6a)** and [MoTp(O)Cl$_2$](μ-O), trans isomer **(6b)**, the peak at 958 cm^{-1} was assigned as Mo=O of the terminal oxo groups [12].

The compound [MoTp*(O)Cl]$_2$(μ-O) **(7)** exhibited $\nu_{(Mo=O)}$ at 960 and 859 cm^{-1}. This value has been reported as 961 and 971 cm^{-1} for [MoTp^{pr}(O)Cl](μ-O) [MoTp^{pr}(O)(OH)] **(19)** (Tp^{pr}= Hydrotris-(3-isopropylpyrazolyl)borate) [28].

The infrared spectrum of the mixed valence compound, [Mo$^{(V)}$Tp*O$_2$](μ-O) [Mo$^{(VI)}$Tp*(O)Cl] **(10)**, exhibited three $\nu_{(Mo=O)}$ bands in the region 850-1000 cm^{-1}. The $\nu_{(Mo=O)}$ bands were assigned to Mo$^{(V)}$=O (955 cm^{-1}) and cis-Mo$^{(VI)}$O$_2$ (925, 895 cm^{-1}) [17].

A detailed infrared and raman spectroscopy study was carried out for the geometric isomers of **(6a)** and **(6b)** [12]. According to this study, the peaks at 784 cm^{-1} and 456 cm^{-1} were assigned to the asymmetric stretch and the deformation mode of the linear oxo-bridged unit, respectively[15]. For the compound [MoTp*(O)Cl]$_2$(μ-O) **(7)**, symmetric stretch oxo-bridged unit was reported as 753 cm^{-1} [29]. Therefore, the peaks observed for the compounds **(I)-(VI)** at ca. 755 cm^{-1} and 455 cm^{-1} could be assigned to asymmetric stretch and deformation mode of the Mo-O-Mo unit, respectively. The presence of the μ-oxo ligand was indicated by a strong, broad ν_{as}(Mo-O-Mo) band at 750 cm^{-1} for the compound [Mo$^{(V)}$Tp*O$_2$](μ-O)[Mo$^{(VI)}$Tp*(O)Cl] **(9)** [17] as well.

The two vibrations at ca. 3370 cm^{-1} and 3450 cm^{-1} from the symmetric and asymmetric stretching modes of the NH$_2$ groups of the free ligands have completely disappeared in the IR spectra of all the new complexes **(I)-(VI)**. The structure determined by the X-ray diffraction analyses revealed a triple bond between molybdenum and nitrogen. McCleverty et al. reported [20] the oxo imido molybdenum compounds [MoTp*(O)Cl(=NR)] **(12)** (R= 4-tolyl, **(12a)** and C$_6$H$_4$NMe$_2$-4, **(12b)**) and [MoTp*(O)Cl]$_2$(NC$_6$H$_4$N) **(13)**. In general, identifying a $\nu_{(Mo=N)}$ or $\nu_{(Mo\equiv N)}$ vibration is a difficult task because of (i) the variability in the Mo-N bond order, and (ii) coupling of

the Mo=N vibration to other vibrations in the molecule, in particular the adjacent N-C vibration of the imido group [30]. However, a value of 1200-1300 cm^{-1} for the $\nu_{(Mo=N)}$ has been suggested [31] and Mccleverty et al. [32] reported values in the range 1200-1250 cm^{-1} for the compounds mentioned above (**12a, 12b, 13**). The IR spectra of the binuclear μ-oxo compounds **(I)-(VI)** also exhibited peaks around 1200-1300 cm^{-1} range which may be ascribed to $\nu_{(Mo≡N)}$.

Table 3.2. Some important IR data for the complexes; (cm^{-1}).

Complexes	ν(BH)	ν(Mo=O)	ν(Mo≡N)
(I)	2548	957	1204
(II)	2548	957	1204
(III)	2549	958	1205
(IV)	2549	958	1205
(V)	2553	952	1208
(VI)	2549	948	1207
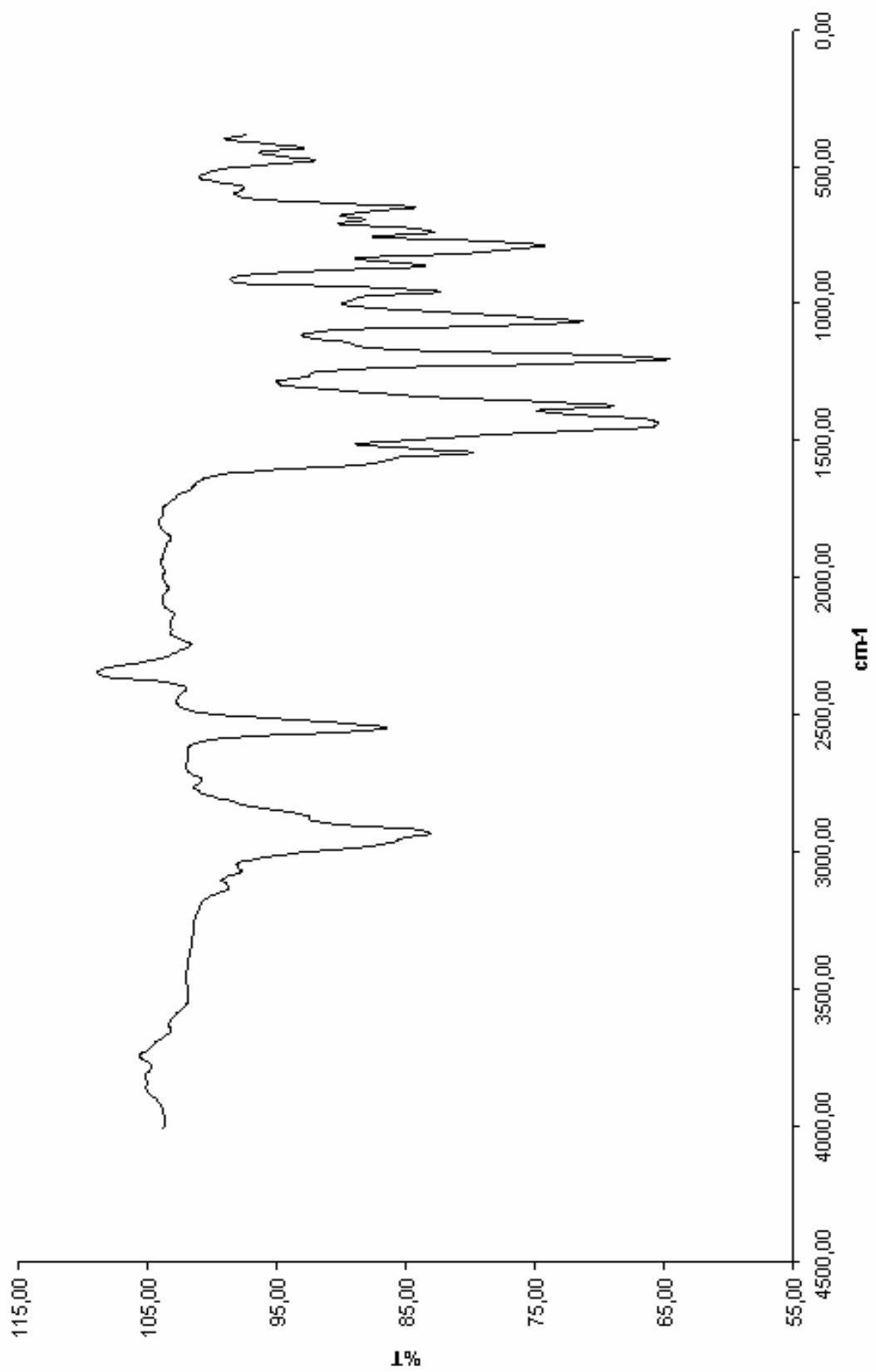
Figure 3.12. The IR spectrum of [MoTp*(O)Cl](µ-O)[MoTp*(Cl)(≡NC₆H₄F)], (I).
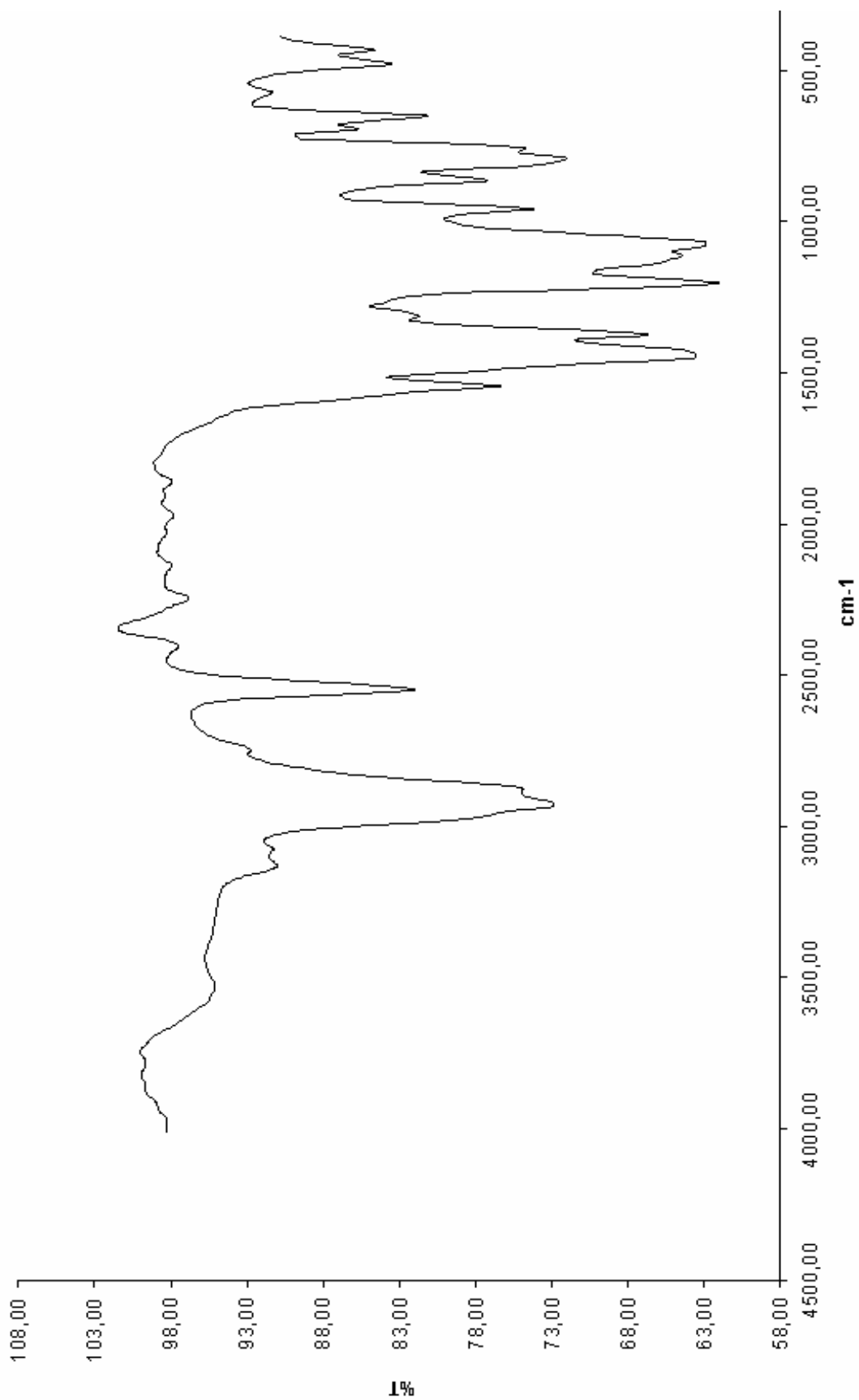
Figure 3.13. The IR spectrum of [MoTp*(O)Cl](μ-O)[MoTp*(Cl)(≡NC₆H₄F)], (II).
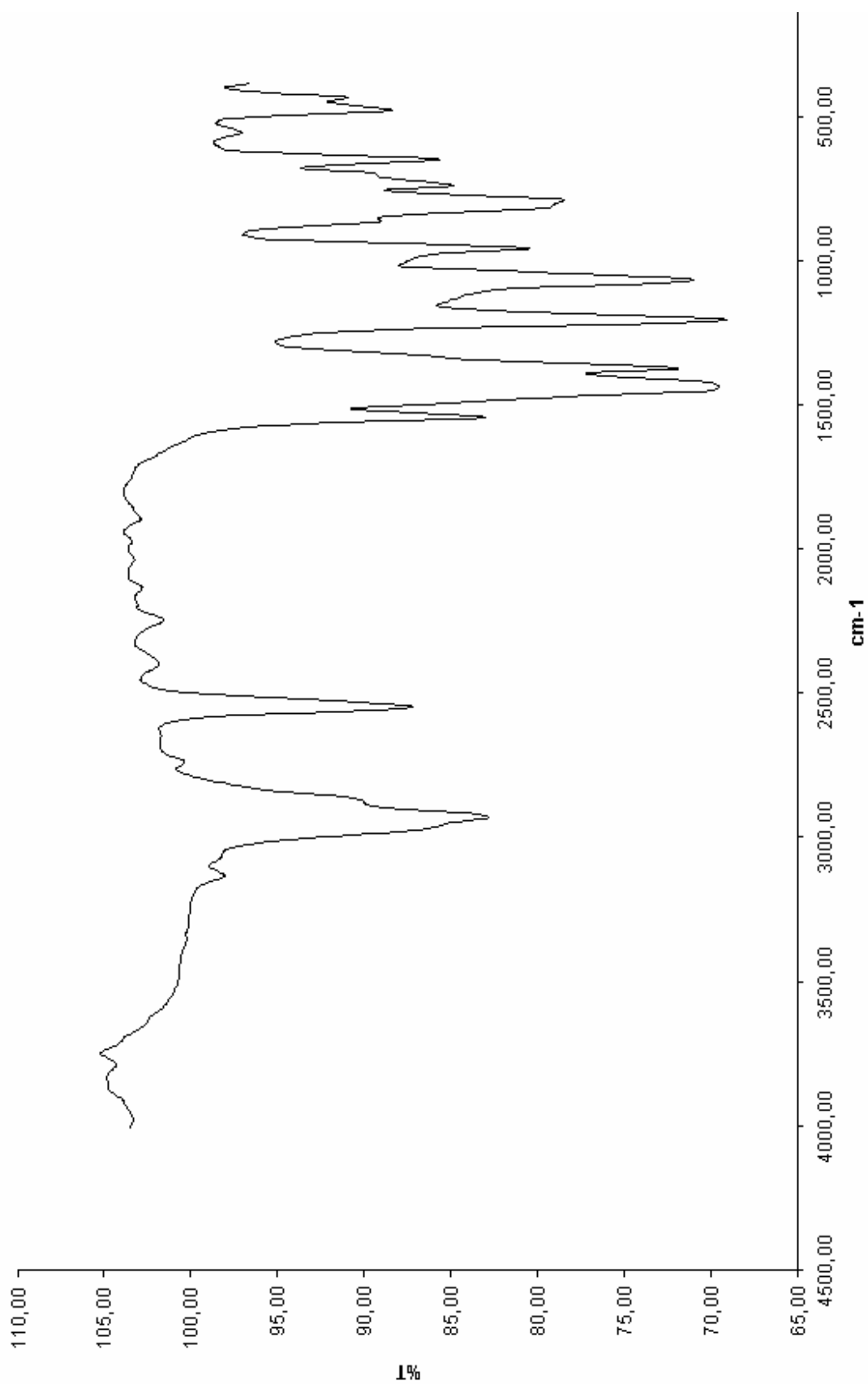
Figure 3.14. The IR Spectrum of [MoTp*(O)Cl](μ-O)[MoTp*(Cl)(≡NC₆H₄Br)], (III).
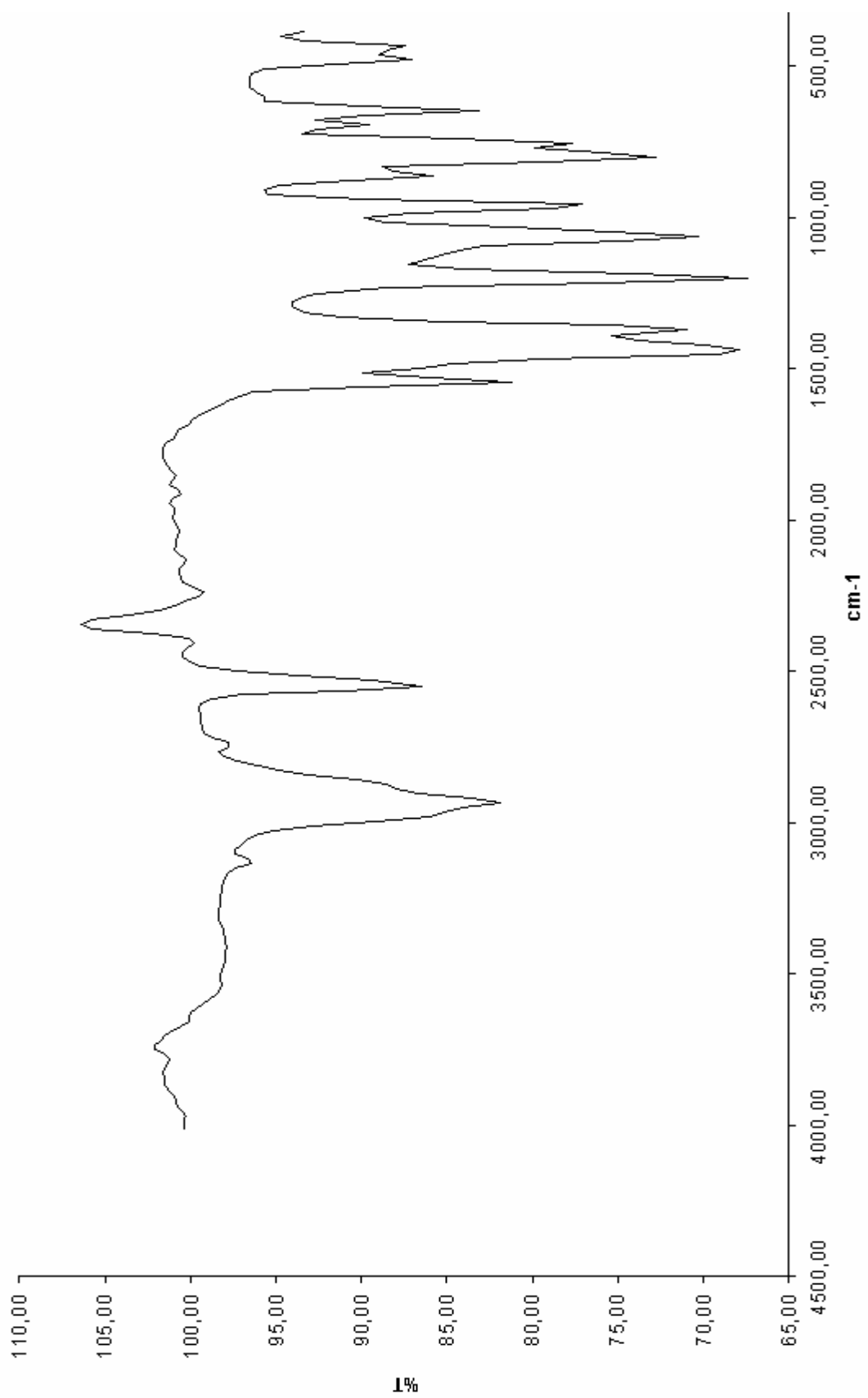
Figure 3.15. The IR Spectrum of [MoTp*(O)Cl](μ-O)[MoTp*(Cl)(≡NC₆H₄Br)], (IV).
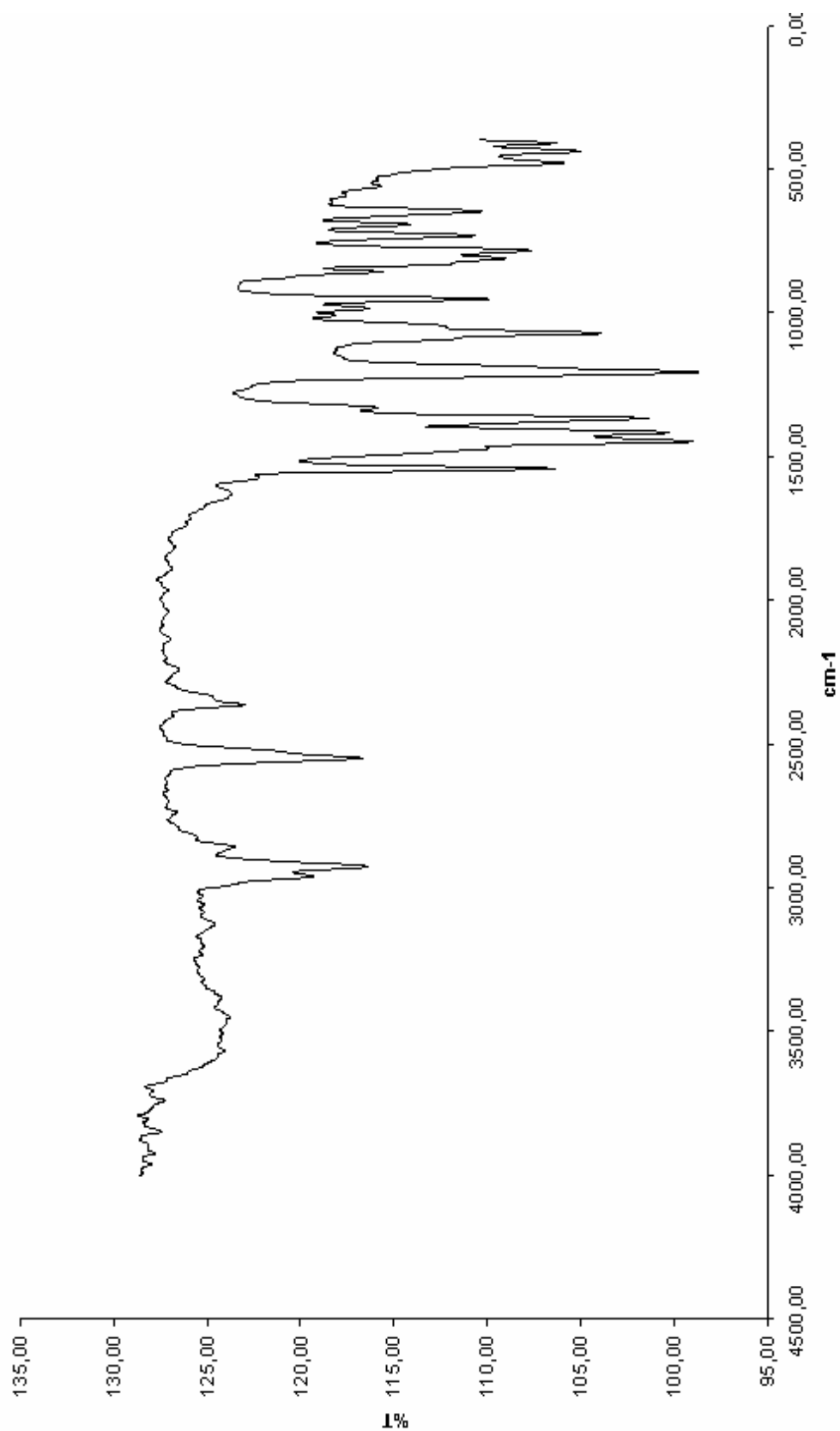
Figure 3.16. The IR Spectrum of [MoTp*(O)Cl](µ-O)[MoTp*(Cl)(≡NC$_6$H$_4$Cl)], (V).
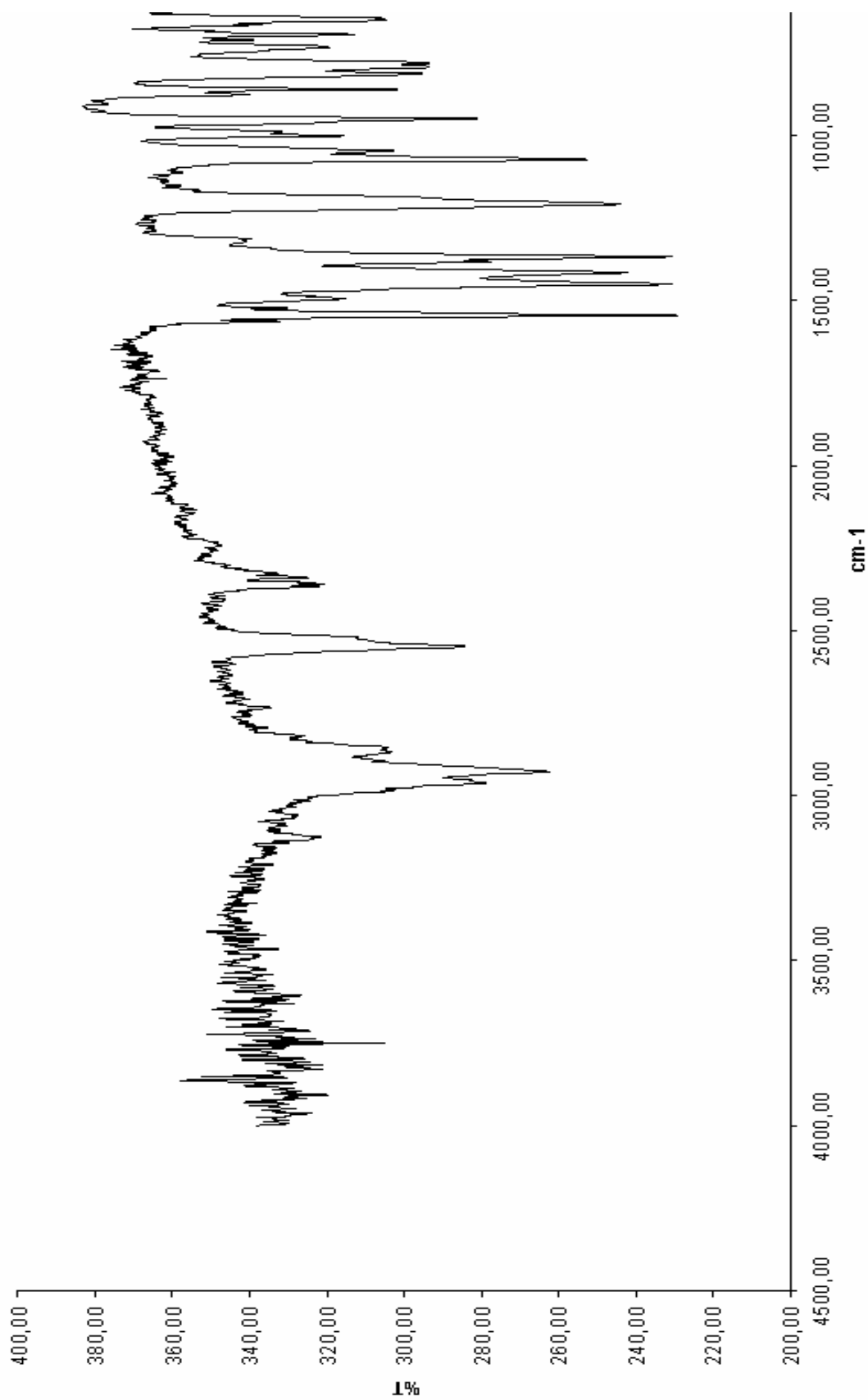
Figure 3.17. The IR spectrum of [MoTp*(O)Cl](μ-O)[MoTp*(Cl)(≡NC₆H₄Cl)], (VI).

35

^{1}H-NMR data for the complexes are given in Table 3.3. and their spectra are shown in Figure 3.18.-3.23

The ^{1}H-NMR spectra of the new complexes **(I)-(VI)** exhibited peaks consistent with structures determined by X-ray diffraction method. The signals attributable to the Tp* ligand appeared as two groups of singlets in the region 1.23-3.56 p.p.m. assigned to the pyrazolyl ring methyl protons and 5.28-6.21 p.p.m. assigned to the pyrazolyl ring C-H protons. In the spectra of **(I)**, **(III)**, **(V)**, **(VI)** six resonances due to the proton on C_4 were observed whereas **(II)** and **(IV)** exhibited three resonances. This indicated three inequivalent H(4) protons and six inequivalent methyl groups for each Tp* ligand in the molecule. The reason for observing three resonances instead of six in **(II)** and **(IV)** could be attributed to accidental degeneracy of the three H(4) resonances for two inequivalent Tp* ligands. This effect has previously been observed by McCleverty et al. [33]. The low symmetry of the molecules means six methyl resonances must be observed in the area of 1.5-3.5 p.p.m. However, it is not easy to make certain assignments in that area for a total of 36 methyl groups (18 Me for each Tp*). All the new complexes exhibited peaks in the region 1.23-3.56 p.p.m. attributable to the Me groups of the Tp* ligand.

Generally NH_2 and NH protons appear in the range δ 11.14-13.15 p.p.m.[34]. No broad signals typical of amine or amide protons were observed in the ^{1}H-NMR spectra of the new compounds **(I)-(VI)** which leads us to beleive that are Mo=N or Mo≡N linkages.

The resonances due to the C_6H_4 protons appeared multiplets in the region δ 6.27-7.39 p.p.m. for the compounds [MoTp*(O)Cl](μ-O)[MoTp*(Cl)(≡NC_6H_4F)] **(I)** and **(II)** and as an A_2B_2 system in the region δ 7.24-7.51 p.p.m. for the compounds **(III)** and **(V)**. Only a single signal has been observed at 7.42 p.p.m. for C_6H_4 protons for the compound **(IV)**. However, the compound **(III)** has been observed one singlet, two doublet and one triplet in the region δ 6.95-7.69 for C_6H_4 protons. This difference could be explained by the difference in position of the functionalized X and Y groups on the aromatic ring.

Table 3.3. ^{1}H-NMR data for the complexes

Complex	δ^b/ p.p.m.	A^c	Assignment
(I)	7.18-7.39	4	m, NC_6H_4
	6.21	1	s, $Me_2C_3\underline{H}N_2$
	6.13	1	s, $Me_2C_3\underline{H}N_2$
	5.97	1	s, $Me_2C_3\underline{H}N_2$
	5.93	1	s, $Me_2C_3\underline{H}N_2$
	5.56	1	s, $Me_2C_3\underline{H}N_2$
	5.52	1	s, $Me_2C_3\underline{H}N_2$
	2.45-3.37	36	$\underline{Me}_2C_3HN_2$
(II)	6.27-6.95	4	m, NC_6H_4
	5.74	2	s, $Me_2C_3\underline{H}N_2$
	5.65	2	s, $Me_2C_3\underline{H}N_2$
	5.62	2	s, $Me_2C_3\underline{H}N_2$
	2.10-3.56	36	$\underline{Me}_2C_3HN_2$

Table 3.3. continued.

Complex	δ^b/ p.p.m.	A^c	Assignment
(III)	7.51	4	A_2B_2, NC_6H_4, $\delta(A)$ 7.56, $\delta(B)$ 7.47
	6.20	1	s, $Me_2C_3\underline{H}N_2$
	6.11	1	s, $Me_2C_3\underline{H}N_2$
	5.97	1	s, $Me_2C_3\underline{H}N_2$
	5.93	1	s, $Me_2C_3\underline{H}N_2$
	5.56	1	s, $Me_2C_3\underline{H}N_2$
	5.51	1	s, $Me_2C_3\underline{H}N_2$
	2.33-3.33	36	$\underline{Me}_2C_3HN_2$
(IV)	7.42	4	s, NC_6H_4
	6.04	2	s, $Me_2C_3\underline{H}N_2$
	5.95	2	s, $Me_2C_3\underline{H}N_2$
	5.68	2	s, $Me_2C_3\underline{H}N_2$
	1.23-3.30	36	$\underline{Me}_2C_3HN_2$

Table 3.3. continued.

Complex	δ^b/ p.p.m.	A^c	Assignment
(V)	7.24	4	A_2B_2, NC_6H_4, $\delta(A)$ 7.32, $\delta(B)$ 7.16
	5.97	1	s, $Me_2C_3\underline{H}N_2$
	5.88	1	s, $Me_2C_3\underline{H}N_2$
	5.74	1	s, $Me_2C_3\underline{H}N_2$
	5.70	1	s, $Me_2C_3\underline{H}N_2$
	5.33	1	s, $Me_2C_3\underline{H}N_2$
	5.28	1	s, $Me_2C_3\underline{H}N_2$
	2.22-3.10	36	$\underline{Me}_2C_3HN_2$
(VI)	7.69	1	s, NC_6H_4
	7.55	1	d, NC_6H_4
	7.41	1	d, NC_6H_4
	6.95	1	t, NC_6H_4
	5.96	1	s, $Me_2C_3\underline{H}N_2$
	5.90	1	s, $Me_2C_3\underline{H}N_2$
	5.77	1	s, $Me_2C_3\underline{H}N_2$
	5.73	1	s, $Me_2C_3\underline{H}N_2$
	5.70	1	s, $Me_2C_3\underline{H}N_2$
	5.31	1	s, $Me_2C_3\underline{H}N_2$
	1.96-2.68	36	$\underline{Me}_2C_3HN_2$

[b] **In CDCl$_3$,** [c] **Relative areas**
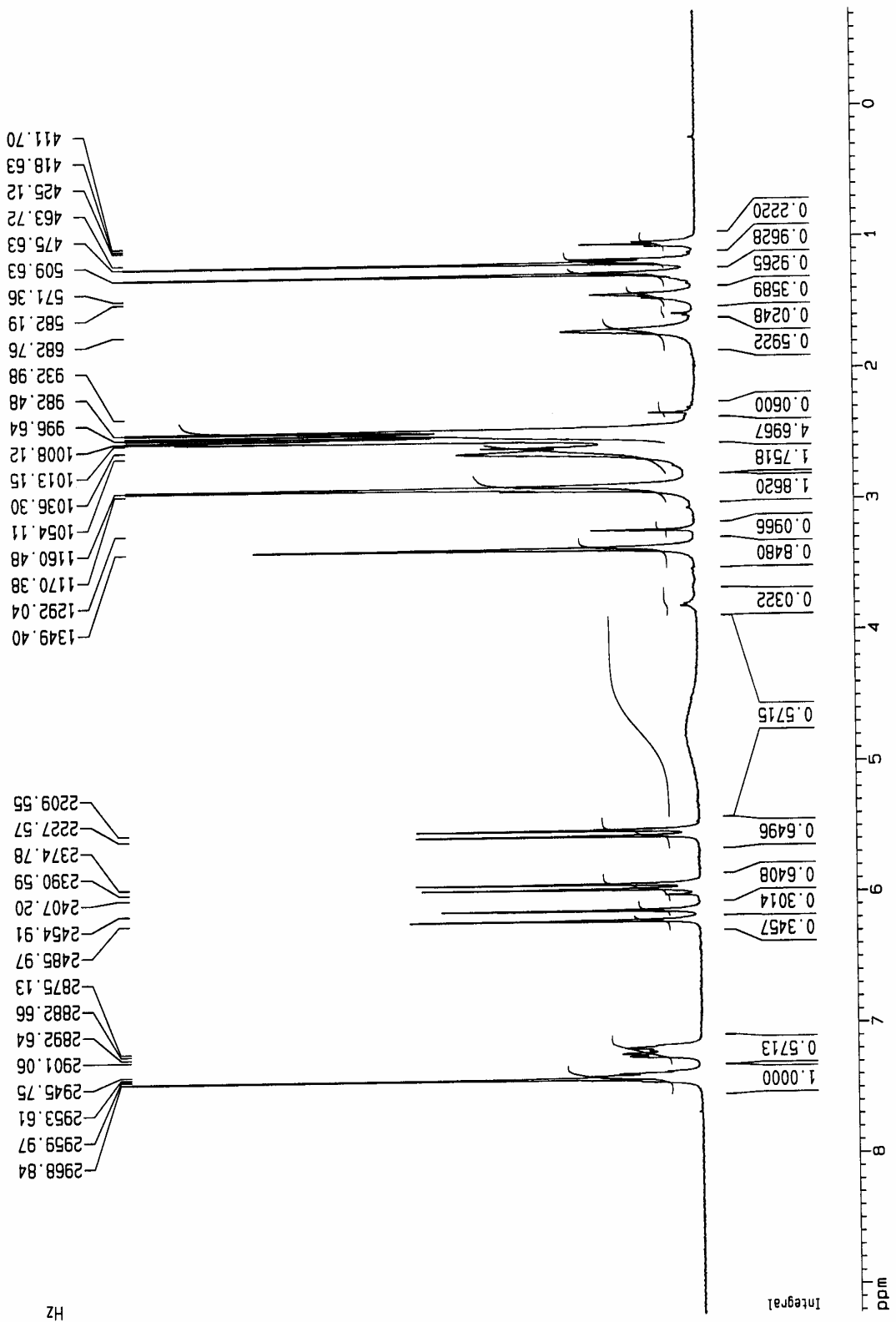
Figure 3.18. The ^{1}H-NMR spectrum of [MoTp*(O)Cl](μ-O)[MoTp*(Cl)($\equiv$NC$_6$H$_4$F)], (I).

Hz

Peak labels (Hz):
411.70, 418.63, 425.12, 463.72, 475.63, 509.63, 571.36, 582.19, 682.76, 932.98, 982.48, 996.64, 1008.12, 1013.15, 1036.30, 1054.11, 1160.48, 1170.38, 1292.04, 1349.40

2209.55, 2227.57, 2374.78, 2390.59, 2407.20, 2454.91, 2485.97, 2875.13, 2882.66, 2892.64, 2901.06, 2945.75, 2953.61, 2956.97, 2968.84

Integral values:
0.2550, 0.9628, 0.9265, 0.3589, 0.0248, 0.5922, 0.0600, 4.6967, 1.7518, 1.8620, 0.0966, 0.8480, 0.0322, 0.5715, 0.6496, 0.6408, 0.3014, 0.3457, 0.5713, 1.0000

Integral

ppm

308.29
388.49
425.02
430.41
436.02
639.76
640.40
671.29
898.69
914.96
925.06
968.81
1087.91
1261.76
1302.33
1324.73
1329.28
1332.28
1338.99
1366.94
1373.11
1383.09
1389.65
1400.47
1419.36
1424.65
1430.73
1436.54
2157.38
2262.71
2262.88
2300.47
2323.29
2510.53
2519.82
2595.43
2716.21
2777.63
2784.15
2877.00

HZ

1.723
4.598
12.733
1.716
11.335
1.116
1.135
1.163
0.525
0.585
0.562
0.562
0.566
0.568
1.082

(x40.0)

ppm

Figure 3.19. The ¹H-NMR spectrum of [MoTp*(O)Cl](μ-O)[MoTp*(Cl)(≡NC₆H₄F)], (II).

41
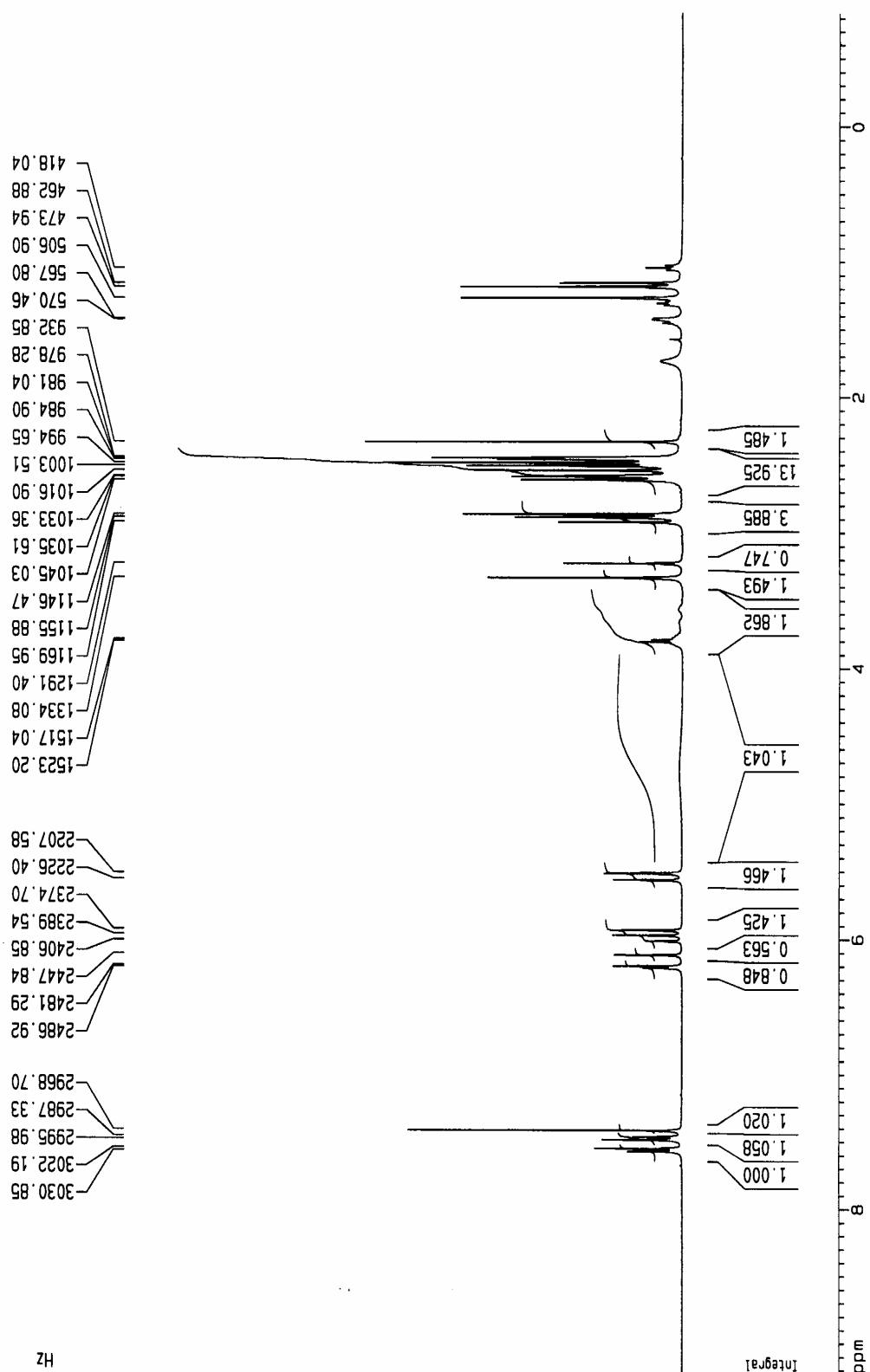
Figure 3.20. The ^{1}H-NMR spectrum of [MoTp*(O)Cl](μ-O)[MoTp*(Cl)($\equiv$NC$_6$H$_4$Br)], (III).

Hz

417.86
496.20
517.52
523.16
528.76
703.87
932.51
992.48
1002.32
1024.15
1167.55
1321.94
1517.48
1523.63
2183.19
2274.96
2381.54
2417.28
2968.65

Integral

0.3192
3.0666
0.8019
0.4666
6.4401
3.2227
3.1885
3.1850
1.8562
0.9952
0.1698
0.9888
0.9999
0.9973
0.6183

ppm
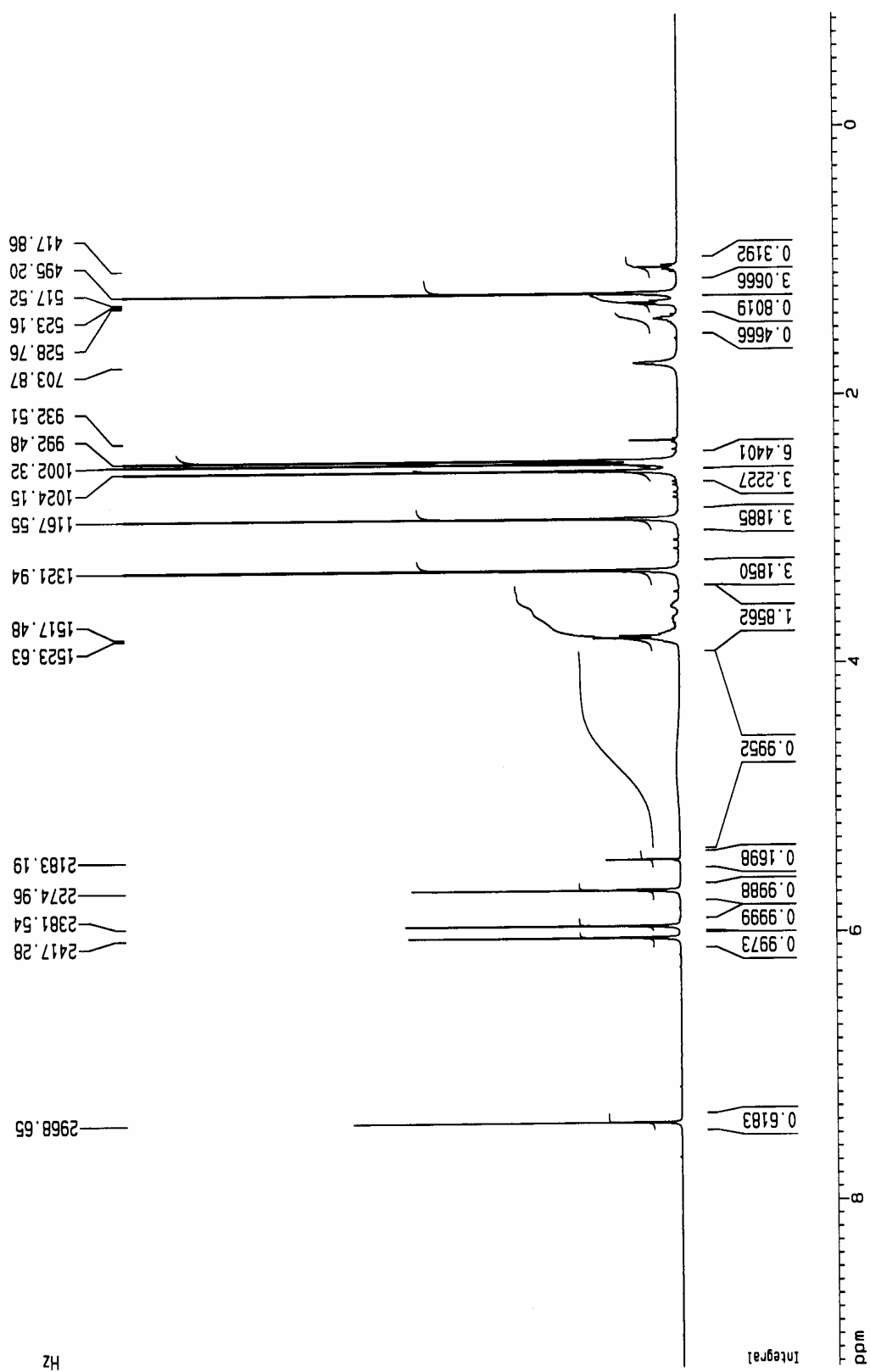
Figure 3.21. The ^{1}H-NMR spectrum of [MoTp*(O)Cl](μ-O)[MoTp*(Cl)($\equiv$NC$_6$H$_4$Br)], (IV).
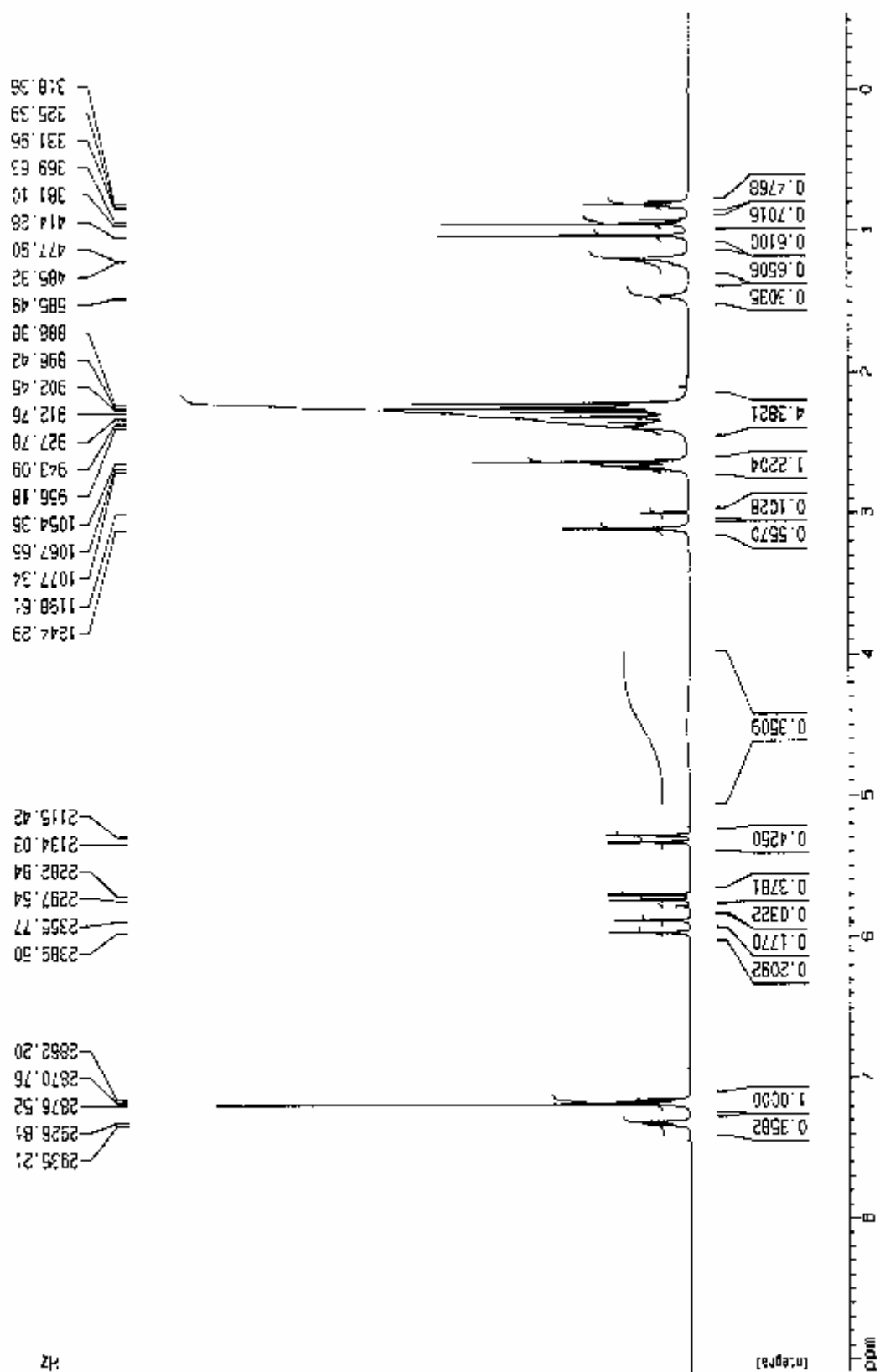
Figure 3.22. The ^{1}H-NMR spectrum of [MoTp*(O)Cl](μ-O)[MoTp*(Cl)($\equiv$NC$_6$H$_4$Cl)], (V).
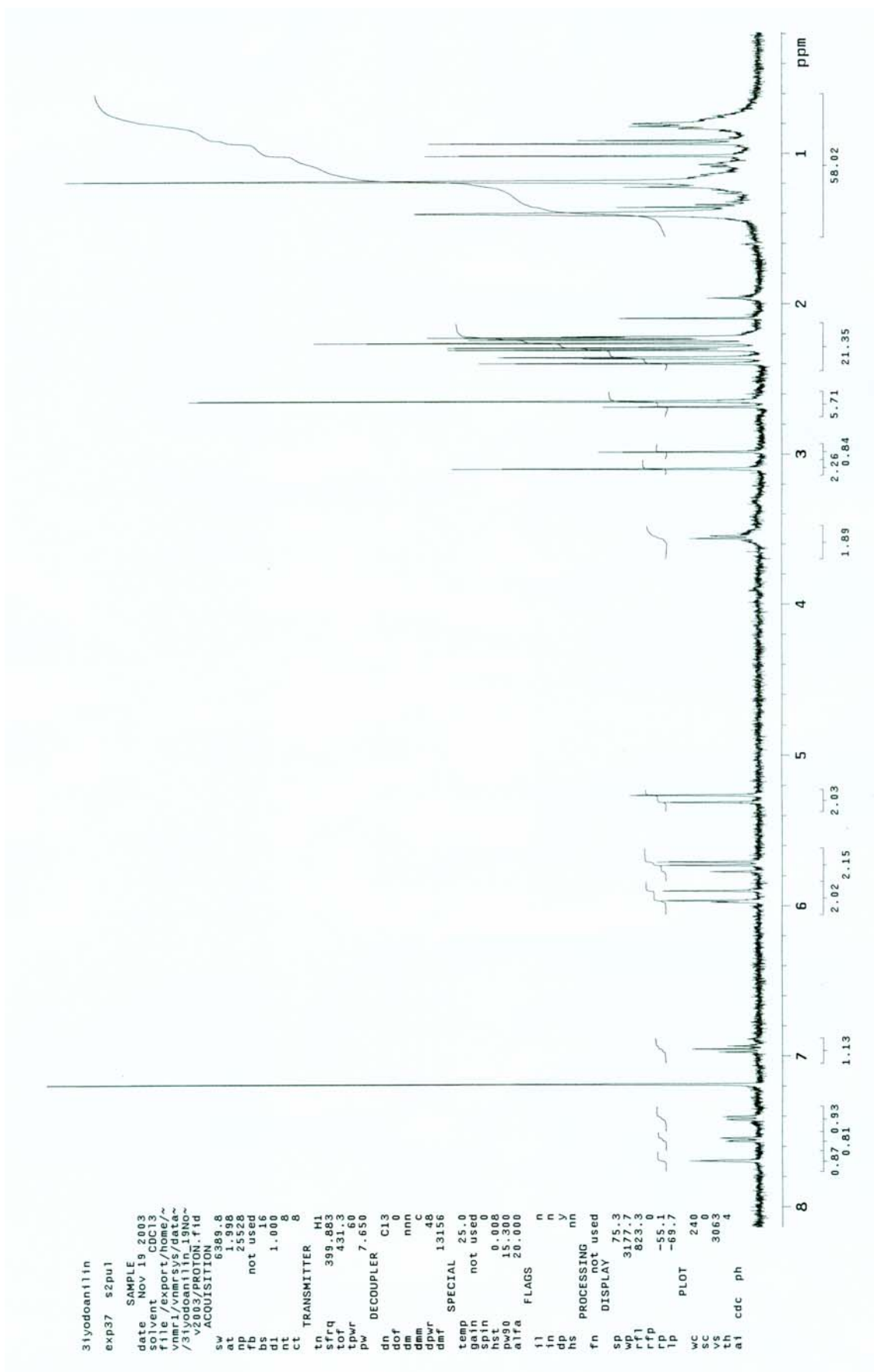
Figure 3.23. The ^{1}H-NMR spectrum of [MoTp*(O)Cl](μ-O)[MoTp*(Cl)($\equiv$NC$_6$H$_4$l)], (VI).

3.2. Crystallographic Studies

The crystal structures of the compounds **(I)**, **(II)**, **(III)**, **(V)**, **(VI)** are shown in Figure 3.25-3.30 and selected bond angles are given in Table 3.4. Crystal data and structure refinement parameters for **(I)**, **(II)**, **(III)**, **(VI)** are given in Table 3.5-3.8.

Binuclear complexes are comprised of two unidentical MoTp*Cl unit connected by a single oxo bridge, there are two pseude-octahedral metal centers. The first metal centers is coordinated by facial Tp*, terminal oxo, terminal chloro and bridging oxo ligand whereas the second is coordinated by facial Tp*, terminal chloro, aryl imido and bridging oxo ligands. It was seen that in **(I)**, **(III)**, **(VI)** two Cl atoms were trans to each other. The structures of the geometric isomers of **(II)** and **(IV)** were also determined to reveal two chlorine atoms bonded in a cis fashion. The reported bond lengths and bond angles for the two geometrical isomers of [MoTp(O)Cl]$_2$(μ-O) **(6a)** [12], [MoTp(O)Cl]$_2$(μ-O) **(6b)** and [MoTp^{pr}(O)Cl](μ-O) [MoTp^{pr}(O)(OH)] **(19)** [28] are all compareble to those encountered here. For instance, the bond angles for the Mo-O-Mo bridging unit in **(I)-(VI)** are close to linear (Table 3.4). The Mo-O-Mo bond angle was reported as 177.3(2) for the compound [MoTp*(O)Cl]$_2$(μ-O) **(7)**. The Mo-O-Mo unit was again close to linear at 177.3(2) for the two geometric isomers of [MoTp(O)Cl]$_2$(μ-O) **(6)** [12]. The distortion from linearity was also observed for the compounds [MoTp*(O)Cl]$_2$(μ-O) **(7)** [29] 177.3(2) and cis-[MoTp(O)Cl]$_2$(μ-O) 177.3(2) [12].

The Mo-N-C bond angles (Table 3.4) are indicative of a linear Mo-N-C(aryl) unit which supports the existance of a triple bond between Mo and nitrogen. Molybdenum nitrogen multiple bond could either be a double bond with Mo-N-C angle of 120° or a triple bond with Mo-N-C angle of 180°.

(a) linear   **(b)** bent

Figure 3.24. Linear (a) and bent (b) imido linkages.

In the case of **(a)** the imido group acts as a six electron donor with no lone pair in the case of **(b)** it behaves as a four electron donor.

Table 3.4. Selected bond lenghts and bond angles

Compound	Mo-O-Mo bond angle	Mo-N-C bond angle
(I)	172.98	161.3
(II)	169.57	178.3
(III)	167.9	176.0
(VI)	168.8	176.3

Table 3.5. Crystal data and structure refinement for compound (I)

Empirical formula	C39 H58 B2 Cl2 F Mo2 N13 O2
Formula weight	1058.39
Temperature	293(2) K
Wavelength	1.54178 Å
Crystal system	Triclinic
Space group	P-1
Unit cell dimensions	a = 10.35260(10) Å α = 96.8230(10)°
	b = 10.85720(10) Å β = 99.7700(10)°
	c = 23.1456(2) Å γ = 96.2990(10)°
Volume	2523.16(4) Å^3
Z	2
Density (calculated)	1.393 Mg/m^3
Absorption coefficient	5.456 mm^{-1}
F(000)	1086
Crystal size	0.12 x 0.12 x 0.1 mm
θ range for data collection	1.96 to 70.06°
Index ranges	-12<=h<=12, -12<=k<=12, -27<=l<=28
Reflections collected	19529
Independent reflections	8505 [R_{int} = 0.0364]
Completeness to θ = 70.06°	88.7 %
Absorption correction	Multi scan
Max. and min. transmission	1.000 and 0.420
Refinement method	Full-matrix least-squares on F^2
Data / restraints / parameters	8505 / 55 / 601
Goodness-of-fit on F^2	S = 1.025
R indices [for 7190 reflections with I>2σ(I)]	R_1 = 0.0429, wR_2 = 0.1190
R indices (for all 8505 data)	R_1 = 0.0488, wR_2 = 0.1222
Weighting scheme	$w^{-1} = \sigma^2(F_o^2) + (aP)^2 + (bP)$,
	where $P = [max(F_o^2, 0) + 2F_c^2]/3$
Largest diff. peak and hole	1.263 and -0.728 eÅ^{-3}

Table 3.6. Crystal data and structure refinement for compound (II)

Empirical formula	C38.50 H53 B2 Cl7 F Mo2 N13 O2
Formula weight	1210.59
Temperature	173(2) K
Wavelength	0.71073 Å
Crystal system	Monoclinic
Space group	P2(1)/n
Unit cell dimensions	a = 12.3726(15) Å $\alpha = 90°$
	b = 25.148(3) Å $\beta = 92.556(2)°$
	c = 16.747(2) Å $\gamma = 90°$
Volume	5205.7(11) Å^3
Z	4
Density (calculated)	1.545 Mg/m^3
Absorption coefficient	0.892 mm^{-1}
F(000)	2452
Crystal size	0.12 x 0.12 x 0.07 mm
θ range for data collection	1.46 to 27.52°
Index ranges	-16<=h<=16, -32<=k<=32, -21<=l<=21
Reflections collected	54997
Independent reflections	11945 [$R_{int} = 0.0771$]
Completeness to $\theta = 27.52°$	99.7 %
Refinement method	Full-matrix least-squares on F^2
Data / restraints / parameters	11945 / 0 / 624
Goodness-of-fit on F^2	S = 1.053
R indices [for 7696 reflections with $I>2\sigma(I)$]	$R_1 = 0.0433$, $wR_2 = 0.1033$
R indices (for all 11945 data)	$R_1 = 0.0924$, $wR_2 = 0.1270$
Weighting scheme	$w^{-1} = \sigma^2(F_o^2) + (aP)^2 + (bP)$,
	where $P = [\max(F_o^2, 0) + 2F_c^2]/3$
Largest diff. peak and hole	1.726 and -1.469 eÅ^{-3}

Table 3.7. Crystal data and structure refinement for compound (III)

Empirical formula	C38 H52 B2 Br Cl5.50 Mo2 N13 O2
Formula weight	1211.31
Temperature	173(2) K
Wavelength	0.71073 Å
Crystal system	Monoclinic
Space group	P2(1)/n
Unit cell dimensions	a = 9.622(3) Å $\alpha = 90°$
	b = 23.426(8) Å $\beta = 99.326(7)°$
	c = 23.703(8) Å $\gamma = 90°$
Volume	5272(3) Å^3
Z	4
Density (calculated)	1.526 Mg/m^3
Absorption coefficient	1.558 mm^{-1}
F(000)	2438
Crystal size	0.2 x 0.2 x 0.1 mm
θ range for data collection	1.94 to 27.51°
Index ranges	-11<=h<=12, -30<=k<=30, -30<=l<=30
Reflections collected	39944
Independent reflections	12012 [$R_{int} = 0.1062$]
Completeness to $\theta = 27.51°$	99.0 %
Refinement method	Full-matrix least-squares on F^2
Data / restraints / parameters	12012 / 40 / 606
Goodness-of-fit on F^2	S = 1.032
R indices [for 6833 reflections with $I>2\sigma(I)$]	$R_1 = 0.0613$, $wR_2 = 0.1414$
R indices (for all 12012 data)	$R_1 = 0.1353$, $wR_2 = 0.1660$
Weighting scheme	$w^{-1} = \sigma^2(F_o^2) + (aP)^2 + (bP)$,
	where $P = [max(F_o^2, 0) + 2F_c^2]/3$
	a = 0.0744, b = 0.0000
Largest diff. peak and hole	1.687 and -1.109 eÅ^{-3}

Table 3.8. Crystal data and structure refinement for compound (VI)

Empirical formula	C45 H65 B2 Cl2 I Mo2 N13 O3
Formula weight	1247.40
Temperature	293(2) K
Wavelength	0.71073 Å
Crystal system	Monoclinic
Space group	P2(1)/c
Unit cell dimensions	$a = 14.785(3)$ Å $\alpha = 90°$
	$b = 10.269(2)$ Å $\beta = 99.89(3)°$
	$c = 36.795(7)$ Å $\gamma = 90°$
Volume	5503.6(19) $Å^3$
Z	4
Density (calculated)	1.505 Mg/m^3
Absorption coefficient	1.164 mm^{-1}
F(000)	2524
Crystal size	0.2 x 0.08 x 0.08 mm
θ range for data collection	1.64 to 27.49°
Index ranges	-19<=h<=19, -13<=k<=13, -47<=l<=47
Reflections collected	62372
Independent reflections	12641 [$R_{int} = 0.0930$]
Completeness to $\theta = 27.49°$	99.9 %
Refinement method	Full-matrix least-squares on F^2
Data / restraints / parameters	12641 / 98 / 635
Goodness-of-fit on F^2	S = 1.137
R indices [for 10029 reflections with I>2σ(I)]	$R_1 = 0.0844$, $wR_2 = 0.1953$
R indices (for all 12641 data)	$R_1 = 0.1078$, $wR_2 = 0.2059$
Weighting scheme	$w^{-1} = \sigma^2(F_o^2) + (aP)^2 + (bP)$,
	where $P = [max(F_o^2, 0) + 2F_c^2]/3$
	a = 0.0739, b = 60.8919
Largest diff. peak and hole	2.791 and -2.690 $eÅ^{-3}$
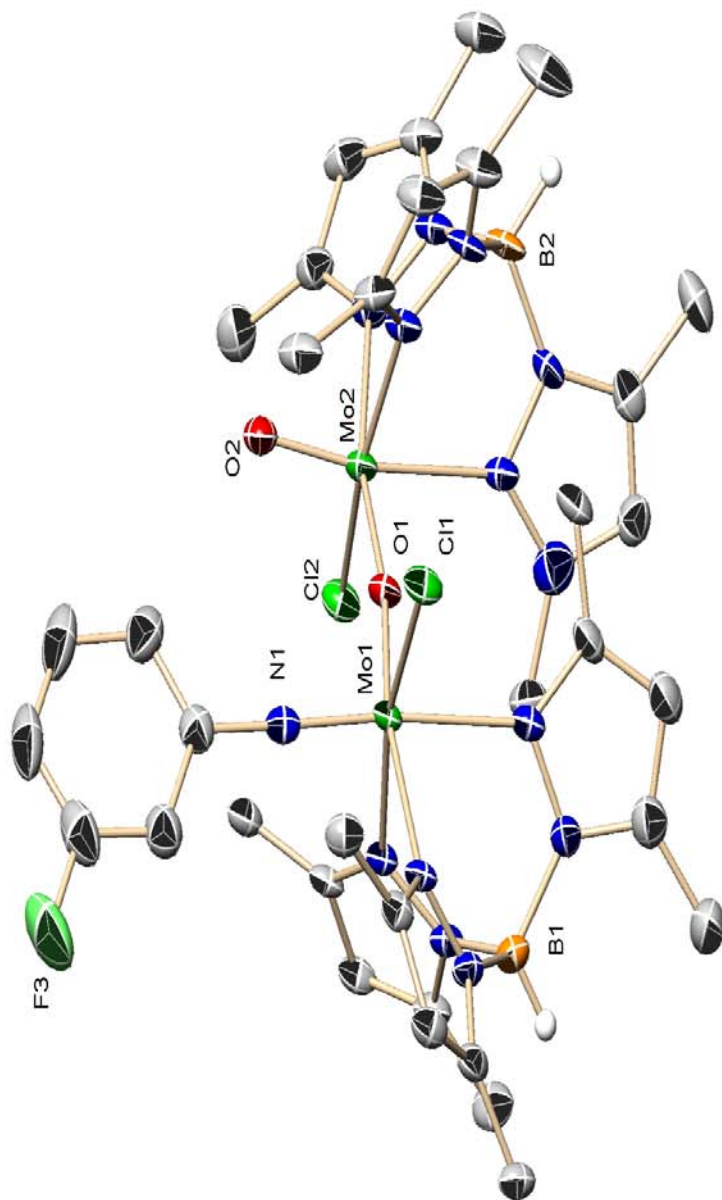
Figure 3.25. The crystal structure of comlex [MoTp*(O)Cl](μ-O)[MoTp*(Cl)(≡NC$_6$H$_4$F)], (I).
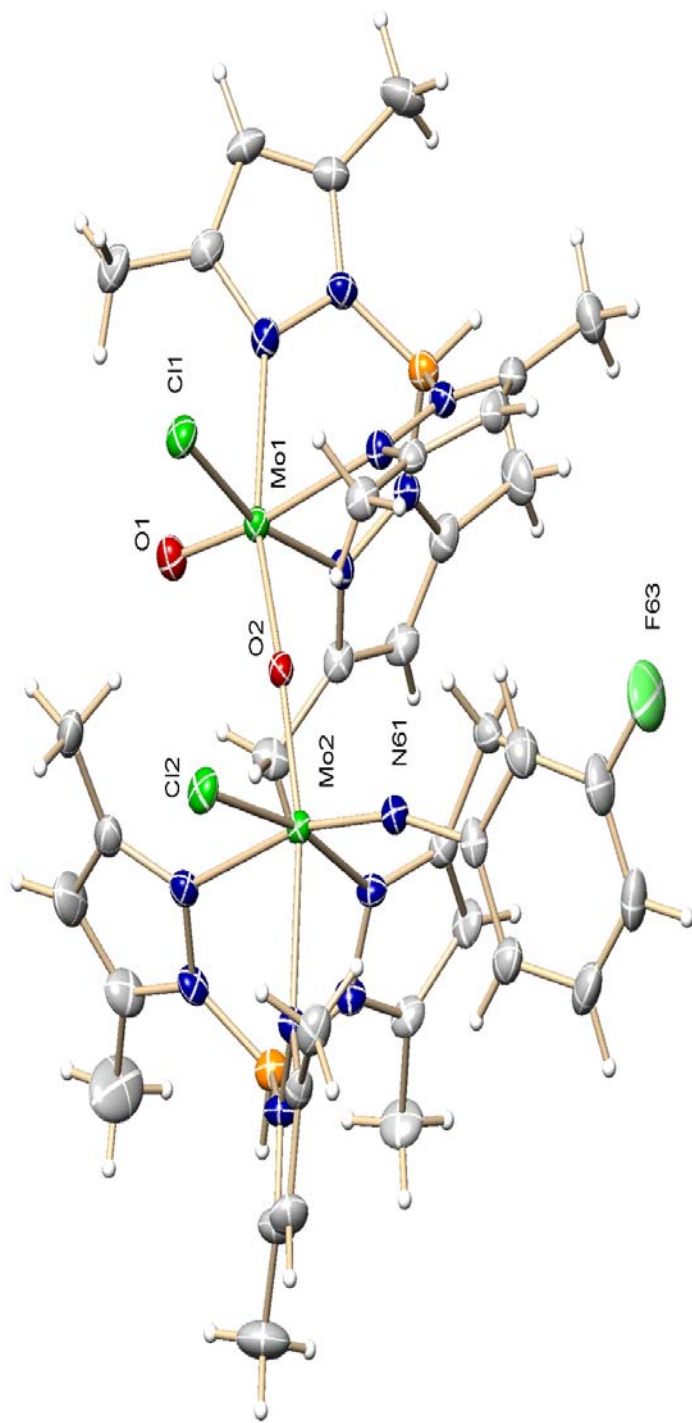
Figure 3.26. The crystal structure of comlex [MoTp*(O)Cl](μ-O)[MoTp*(Cl)(≡NC₆H₄F)], (II).
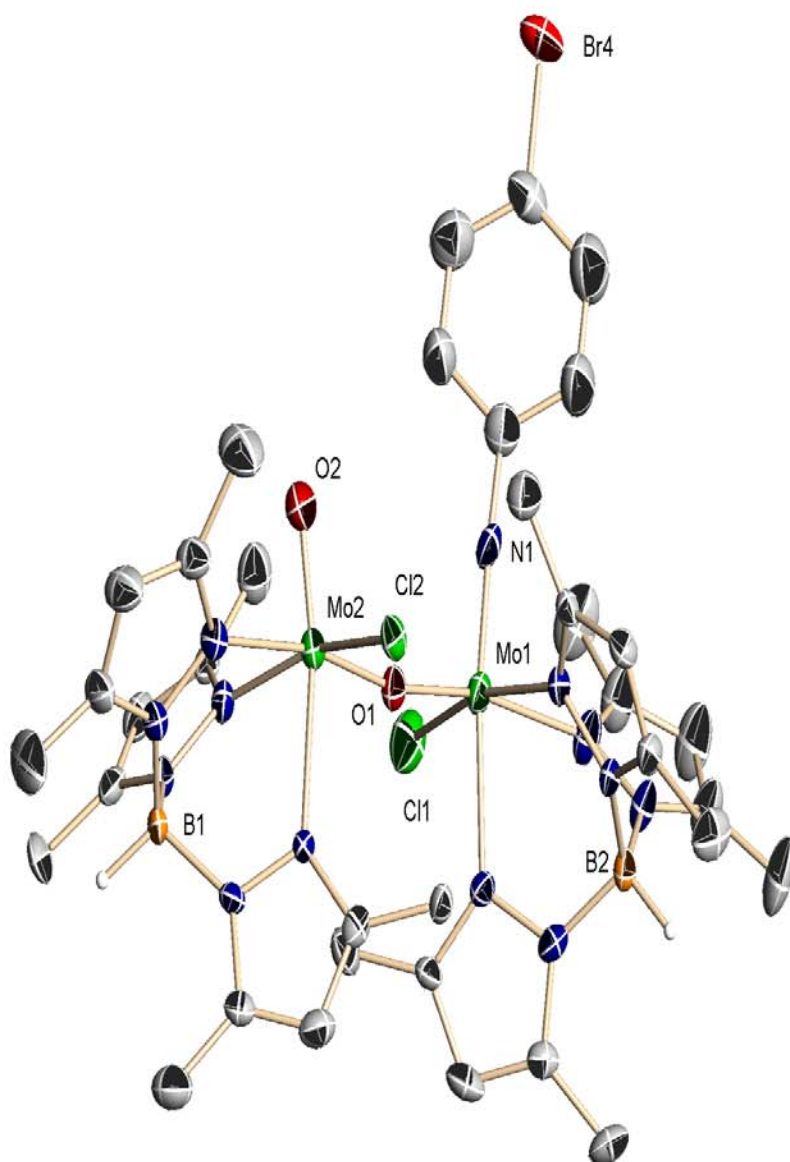
Figure 3.27. The crystal structure of comlex [MoTp*(O)Cl](µ-O)[MoTp*(Cl)(≡NC₆H₄Br)], (III).
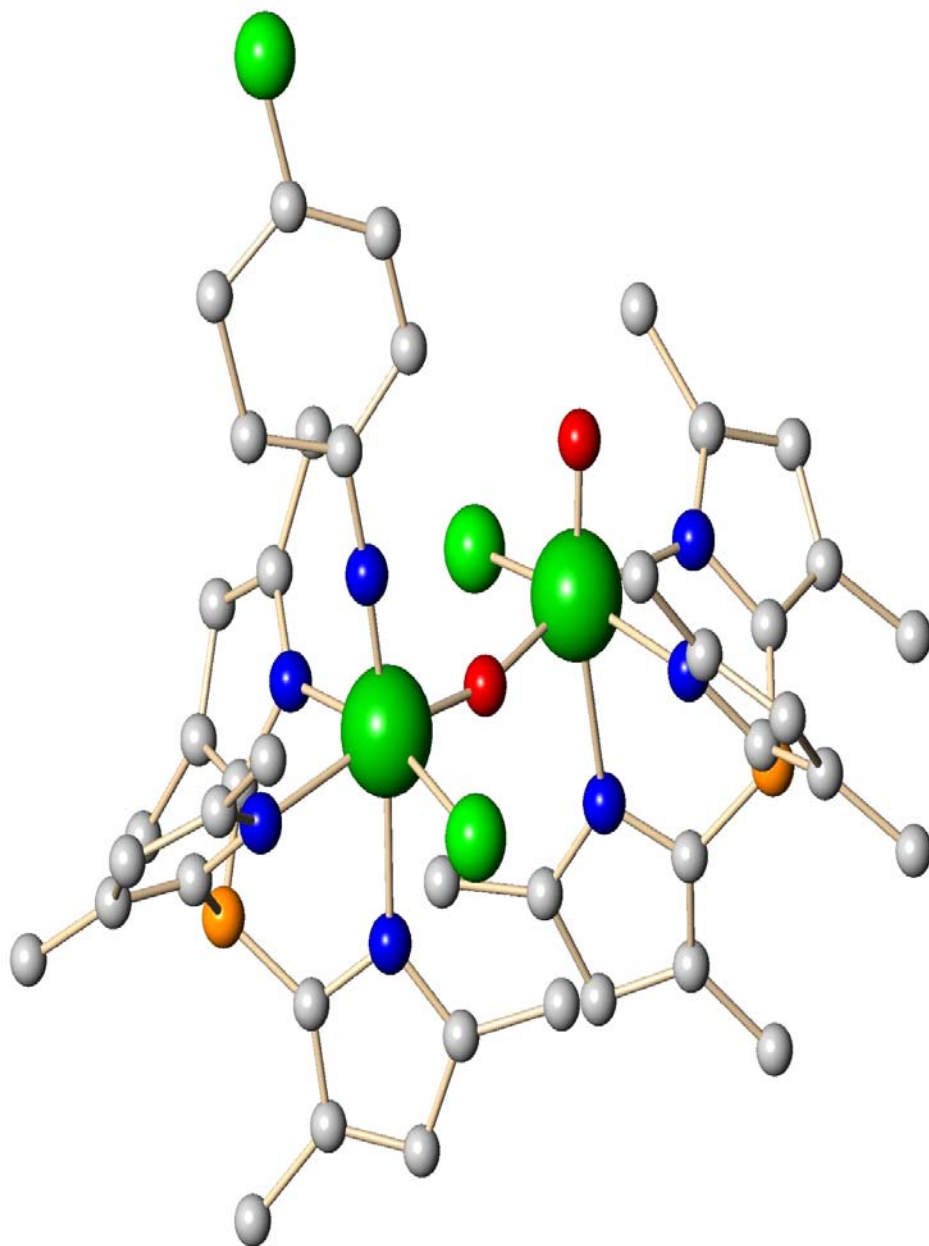
Figure 3.28. The crystal structure of comlex [MoTp*(O)Cl](µ-O)[MoTp*(Cl)(≡NC₆H₄Cl)], (V).
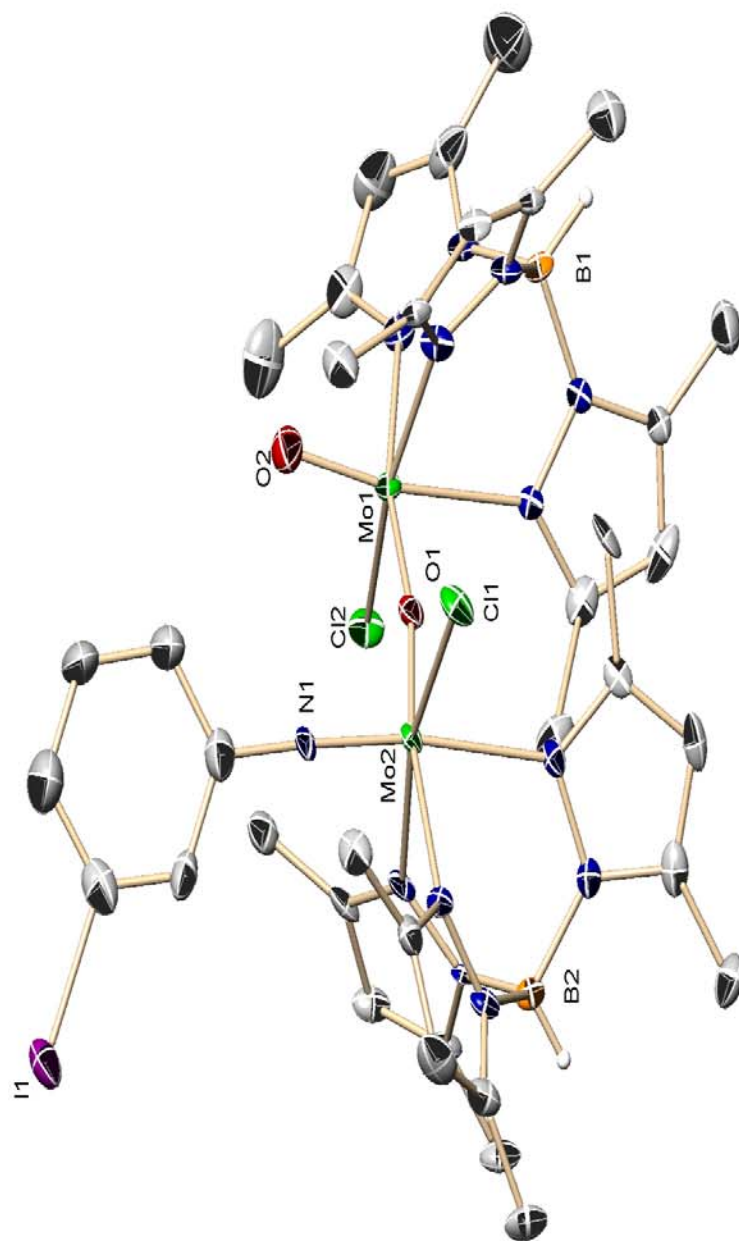
Figure 3.29. The crystal structure of comlex [MoTp*(O)Cl](μ-O)[MoTp*(Cl)(≡NC₆H₄l)], (VI).

Chapter 4

CONCLUSION

The formation of dinuclear oxo bridged imido complexes **(I)-(VI)** from the oxo molybdenum (V) precursor by double deprotonation of amines is of interest and quite unexplored. This represents an entirely new route into oxo-imido-trispyrazolylborate-Mo(V) chemistry. The fallowing synthetic route for the formation of new compounds **(I)-(Vl)** could be suggested (Scheme 4.1.). For simplicity only the formation of $[MoTp*(O)Cl](\mu\text{-}O)[MoTp*(Cl)(\equiv NC_6H_4F)]$ **(I)** are given.
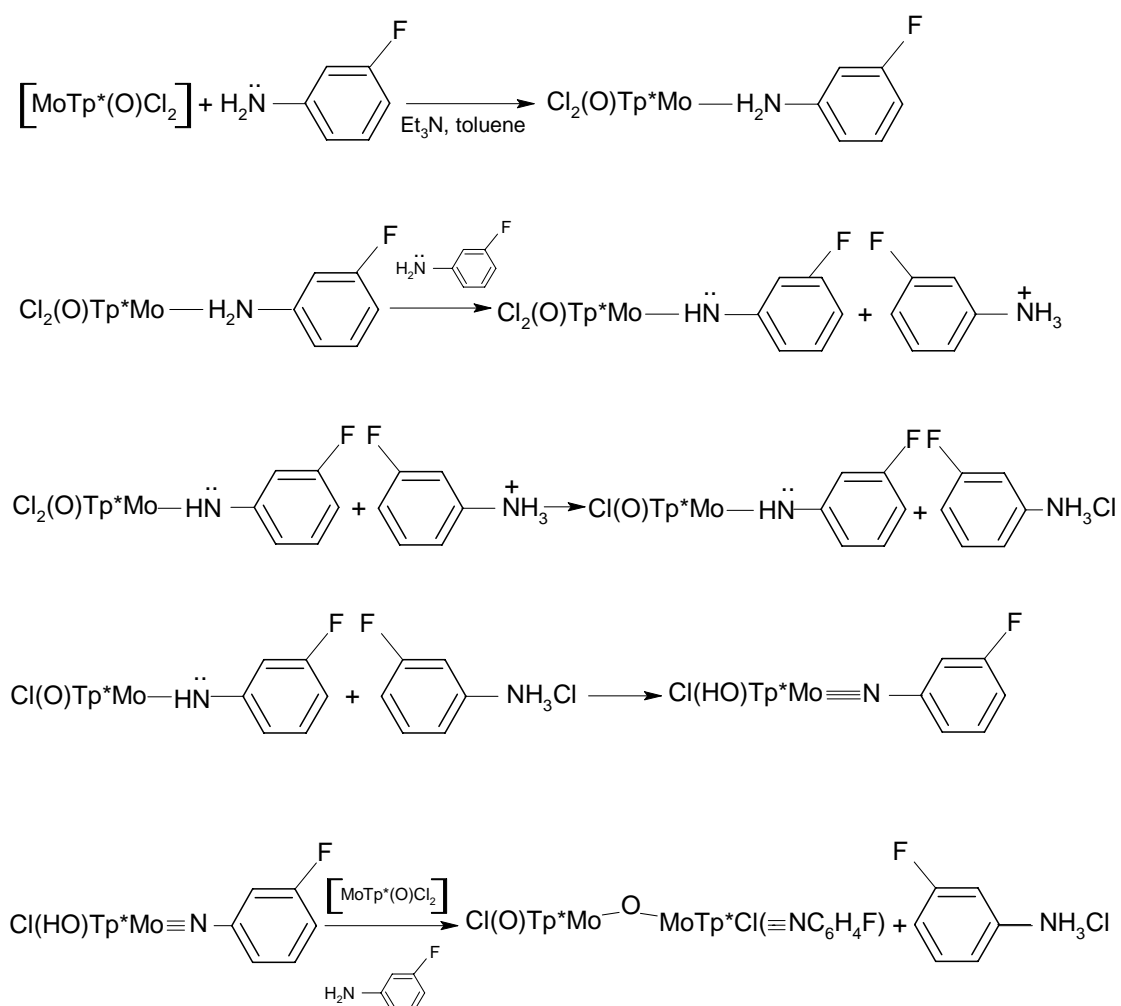
Scheme 4.1. Synthetic route for the formation of compound (I)

REFERENCES

[1]   S. Trafimenko, *J. Am. Chem. Soc.*, **89**, (1967), 3170 and 6288.

[2]   S. Trafimenko, J. P. Jesson, and D. R. Eaton, *J. Am. Chem. Soc.*, **89**, (1967),   3148.

[3]   S. Trafimenko, *J. Am. Chem. Soc.*, **89**, (1967), 4948.

[4]   S. Trafimenko, *Chem. Rev.* **72**, (1972), 487.

[5]   S. Trafimenko, *Accounts Chem. Res.*, **4**, (1971), 17.

[6]   S. Trafimenko, *J. Am. Chem. Soc.*, **91**, (1969), 588.

[7]   J. A. McCleverty and D. Seddon, *J. C. D. Dalton*, (1972), 2526.

[8]   T. A. James and J. A. McCleverty, *J. Chem. Soc.* (A), (1970), 3308. J. A. McCleverty and D. Seddon, *J. Chem. Soc.*, *Dalton Trans.*, (1972), 2526.

[9]   D. Seddon, W.G. Kita, J. Bray and J. A. McCleverty, *Inorg. Synth.*, **16**, (1976), 24.

[10]   S. Trafimenko, *Inorg. Chem.* **10**, (1971), 504.

[11]   M. Millar, S. Lincoln, A.S. Koch, *J. Chem. Soc.*, **104**, (1982), 288.

[12]   S. Lincoln, A.S. Koch, *Inorg. Chem.*, **25**, 1986**,** 1594-1602.

[13]   R.L. Melby, *Inorg. Chem.*, **8**, (1969), 349.

[14]   E.I. Stiefel, *Prog. Inorg. Chem.*, **22**, (1977), 1-223 and references there in.

[15]   S. Lincoln, T.M. Loehr, **29**, (1990), 1907-1915.

[16]   S.A. Roberts, C.G. Young, C.A. Kipke, W.E Cleland, K. Yamanouchi, M.D. Carducci, J.H. Enemark, *Inorg. Chem.*, **29**, (1990), 3650.

[17]   A. Eagle, F. Mackoy, G. Young, *Inorg. Chem.*, **30**, (1991), 1425-1428.

[18]   W.E. Cleland, K.M. Barnhart, K. Yamanouchi, D. Collision, F.E. Mabss, R.B. Ortega, J.H. Enemark, *Inorg. Chem.*, **26**, (1987), 1017-1025.

[19]   B. Spivack, Z. Dori, *Coord. Chem. Rev.*, **17**, (1975), 99.

[20]   Siu-Ming Lee, Ralph Kowallick, Massimo Marcaccio, J. A. McCleverty, M.D. Ward, *J. Chem. Soc.*, *Dalton Trans*., (1998), 3443-3450.

[21]   David A. Bardwell, J.C. Jeffery, John P. Maher, J. A. McCleverty, M.D. Ward, Andrew Williamson, *Inorg. Chem.* **35**, (1996), 5290-5299.

[22]   Samantha Couchman, J.C. Jeffery, J. A. McCleverty, M.D. Ward, Federico Totti and Dante Gatteschi, *Inorg. Chem.*, **38**, (1999), 365-369.

[23]   D. F. Shriver, *The Manipulation of Air-Sensitive Compounds*, *McGraw-Hill, New York*, (1969).

[24]   W. Schlenk and A. Thal, *Chem. Ber.* **46**, (1913), 2843.

[25]   C. J. Barton, *In Techniques of Inorganic Chemistry, Vol. III, H. B. Jonassen and A. Weissberger, eds., Wiley-Interscience, New York*, (1963).

[26]   J. Leonard, B. Lygo, G. Procten, *Advanced Practical Organic Chemistry, published by Blackie Academic & Professional, an imprint of champan & Hall*, (1995).

[27]   L. M. Harwood, C. J. Moody, *Experimental Organic Chemistry, Universty of Oxford*.

[28]   A. Miller, C. Doonan, L. Laughlin, C. Young, *Inorganica Chimica Acta*, **337**, (2002), 393-406.

[29]   M.B. Kassim, R. Paul, J. C. Jeffery, J. A. McCleverty, M.D. Ward, *Inorganica Chimica Acta*, **327**, (2002), 160-168.

[30]   D.E. Wigley, *Prog. Inorg. Chem.*, **42**, (1994), 239 ; W.A Nugent and B. Haymore, *Coord. Chem. Rev.*, **31**, (1980), 123.

[31]   K. Dehnicke and J. Strahle, *Angew. Chem.*, *Int. Ed. Engl.*, **20**, (1981), 413.

[32]   R. Kowallick, M. Marcaccio, J. A. McCleverty and M.D. Ward, *J. Chem. Soc.*, *Dalton Trans.*, (1998), 3443-3450.

[33]   C.J. Jones, J. A. McCleverty, B.D. Neaves and Sarah J. Reynolds, *J. Chem. Soc.*, *Dalton Trans.*(1986), 733-741.

[34]   J. A. McCleverty, G. Denti and S. Reynolds, *J. Chem. Soc.*, *Dalton Trans.*, (1983), 81-89.